Supporting Information

***Rec. Nat. Prod*. 14:6 (2020) 410-415**

Antioxidants and α-Glucosidase Inhibitors from *Lactuca serriola* L.

Nouran H. Abdel Fatah[1], Yhiya Amen[1], Fatma M. Abdel Bar[1, 2], Ahmed F. Halim[1] and Hassan-Elrady A. Saad[1]

[1]Department of Pharmacognosy, Faculty of Pharmacy, Mansoura University, Mansoura 35516, Egypt
[2]Department of Pharmacognosy, Faculty of Pharmacy, Prince Sattam Bin Abdulaziz University, Al-Kharj 11942, Saudi Arabia

Table of Contents — **Page**

1. Experimental and Chemistry

1.1. General experimental

Infra-red spectra were recorded on IR spectrophotometer (Perkin-Elmer 1430 ratio recording). HR-ESI mass spectra were determined using LC-TOF-MS (Shimadzu, Tokyo, Japan), HR-FAB-MS was determined using JEOL JMS 700 spectrophotometer (JEOL, Japan). NMR spectra was recorded on Bruker Ascend^{TM} spectrometer (Bruker Daltonics, Bremen, Germany) at 400 MHz for ^{1}H and 100 MHz for ^{13}C, Bruker Advance DPX spectrometer (Bruker Daltonics Inc., MA, USA) at 600 MHz for ^{1}H and 200 MHz for ^{13}C and JEOL Eclipse NMR spectrometer at 500 MHz for ^{1}H; 125 MHz for ^{13}C where Chemical shifts were obtained I part per million (ppm) on the δ scale with reference to the TMS resonance. Thin layer chromatography was performed on precoated silica gel 60 GF_{254} (20× 20 cm, 0.2 mm thick) on aluminum sheets and precoated RP-C18 F_{254} plates (5 x 7.5 cm x 0.2 mm thick) on aluminium sheets (Merck Co., Darmstadt, Germany). Column chromatography was carried out using silica gel G 60-230 (Merck, Germany) packed by the wet method in the stated solvent, reversed phase chromatography using phase-bonded octadecylsilyl-silica gel (RP-C18, Merck, Germany), Sephadex LH 20 (Pharmacia Fine Chemicals, Sweden) and Diaion HP 20 (Mitsubishi Chemical Corporation, Japan). All the solvents used in column chromatography were purchased from El-Nasr Co. for Pharmaceutical Chemicals, Egypt. and Biochem Co. , Egypt. Azino-bis-(3-ethyl benzthiazoline-6-sulfonic acid) (ABTS), DPPH (2,2-diphenyl-1-picryl-hydrazyl-hydrate), TPTZ (2,4,6-tripyridyl-S-triazine), Trolox (6-hydroxy-2,5,7,8-tetramethyl chromane 2-carboxylic acid), *α*-glucosidase (Saccharomyces cerevisiae) and 3, 5 di-nitro salicylic acid (DNS) were obtained from sigma co., St. Louis, USA. Ascorbic acid (Cevarol®) tablets was obtained from Memphis Pharmaceutical Co., Cairo, Egypt. P-nitro-phenyl-α-D-glucopyranoside (p-NPG), sodium carbonate ($Na_2 CO_3$), sodium dihydrogen phosphate, di-sodium hydrogen phosphate were purchased from Hi-Media, Mumbai, India. All the other chemicals and reagents used in the experiments were of analytical grade and were purchased from El-Nasr Co. for Pharmaceutical Chemicals, Egypt.

1.2. Extraction and isolation:

The air dried powdered aerial parts of *Lactuca serriola* at the flowering stage (1Kg) were extracted by maceration with methanol 90% (7 × 2 L). After removal of the solvent under reduced pressure, the extract (180 g; 18% yield) was partitioned by petroleum ether, methylene chloride, ethyl acetate, and finally by *n*-butanol. The pet. ether fraction (34.94 g) was separated by column chromatography (CC) on silica gel column (78 × 4.5 cm, 500 gm) using a stepwise gradient elution from 100% pet. ether to 100% EtOAc. The effluent was collected in 250 mL fractions into (Fr. 1- 173). Fraction **A** (Fr. 26-29) eluted with pet. ether: EtOAc (92: 8) was left for crystallization to yield **1** (2.3 g). Fraction **B** (Fr. 39-44) eluted with pet. ether: EtOAc (90:10) was allowed to crystallize using CH_2Cl_2/MeOH (2:1) mix. to

yield **2** (120 mg). Fraction **C** (Fr. 83-86) eluted with pet. ether: EtOAc (82:18) was left for crystallization to give powder of **3** (12 mg). Fraction **D** (Fr. 130-140; 400 mg**)** eluted with pet. ether: EtOAc (60:40) was rechromatographed over silica gel column (40 × 1.5 cm) with CH_2Cl_2: EtOAc (88:12) to give **4** (26 mg). Fraction **E** (Fr. 167-169) eluted with pet. ether: EtOAC (10:90) was left for crystallization to give **5** (8 mg).

The methylene chloride fraction (10.42 g) was chromatographed using silica gel column (100 × 3.5 cm, 375 gm) by gradient elution from 100% CH_2Cl_2 to 100% MeOH. The effluent was collected in 100 mL fractions into (Fr. 1- 287). Fraction **F** (Fr. 101-116; 263.6 mg) eluted with CH_2Cl_2: MeOH (98:2) was applied repeatedly over silica gel column (40 × 1.5 cm) with CH_2Cl_2: EtOAc (90:10) to give **6** (12 mg). Fraction **G** (Fr. 122-141; 231 mg) eluted with CH_2Cl_2: MeOH (98:2) was rechromatographed over silica gel column (35 × 1.5 cm) in isocratic manner using methylene chloride (100%) and collecting 15 mL each fraction to elute 1 (subfraction 21-25) & 2 (subfraction 80-100). These subfractions were further purified over sephadex LH20 column (40 × 1 cm) with MeOH to give **8** (2 mg) & **9** (11 mg) respectively. Fraction **H** (Fr. 185-213) eluted with CH_2Cl_2: MeOH (97:3) was washed with CH_2Cl_2 and MeOH to yield powder of **7** (25 mg).

The EtOAc fraction (15.47 g) was loaded over silica gel column (90 × 3.5 cm, 300 gm) starting with pet. ether: EtOAc 80:20% then increasing gradient to 100% EtOAc to 100% MeOH. The effluent was collected in 250 mL fractions into (Fr. 1- 168). Fraction **I** (Fr. 10-14; 785.6 mg) eluted with pet. ether: EtOAc (60:40) was applied over silica gel column (38 × 1.5 cm) to elute (**1'-3'**) subfractions with isocratic elution using CH_2Cl_2: EtOAc (93:7) and collecting 15 mL each fraction. Subfraction **1'** (70-78) was further purified on sephadex LH20 column (22 × 1 cm) with MeOH (97:3) to yield **10** (11 mg). Sephadex LH20 column (20 × 1 cm) was used for subfraction **2'**(80-90) purification to yield **11** (4 mg) with MeOH. Subfraction **3'(**105-199) was rechromatographed over sephadex LH20 column (25 × 1 cm) with MeOH to yield **12** (3 mg) & **13** (5 mg) respectively. Fraction **J** (Fr. 83-90) was left for recrystallization from methanol to yield **15** (21 mg). The remaining part after crystallization was purified over sephadex LH20 column (36 × 1 cm) with CH_2Cl_2: MeOH (99:1) to yield **14** (7 mg).

The *n*-butanol fraction (15 g) was applied over Diaion HP 20 column (40 × 4.5 cm, 120 gm). The effluent was collected in 1000 mL fractions into (Fr. 1- 10). Fraction **K** (Fr. 3-4; 2.6 gm) eluted with H_2O: MeOH (70:30)& (60:40) was re-chromatographed over Diaion HP 20 column (50 × 1.5 cm, collecting 100 mL fractions). Fraction (20-39) eluted with H_2O: MeOH (93:17) was purified repeatedly over Sephadex LH20 column (38 × 1 cm) with MeOH to elute **16** (4mg), **17** (4.3 mg) respectively.

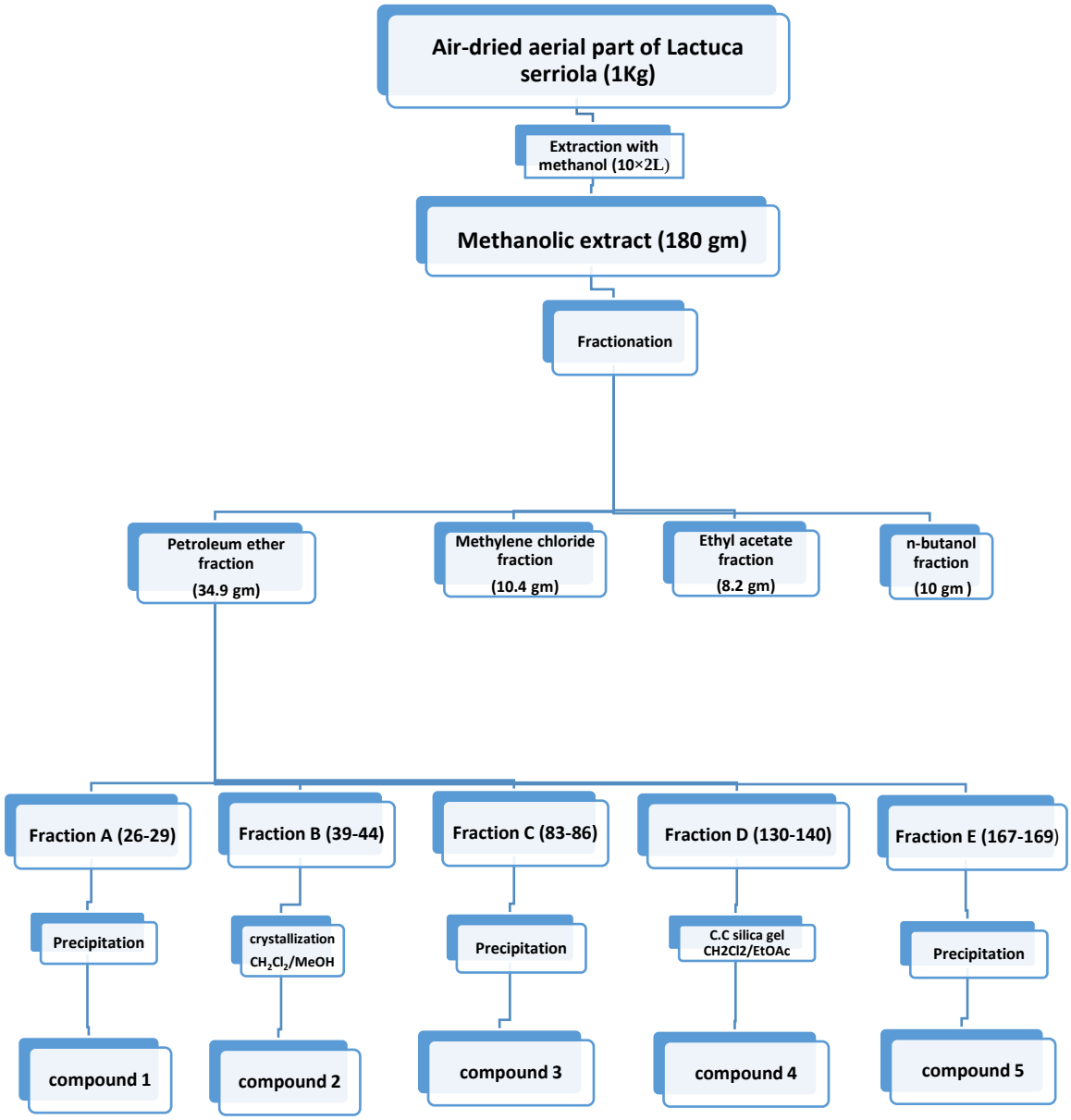

Flowchart 1: Phytochemical investigation of petroleum ether fraction of aerial part of *Lactuca serriola*

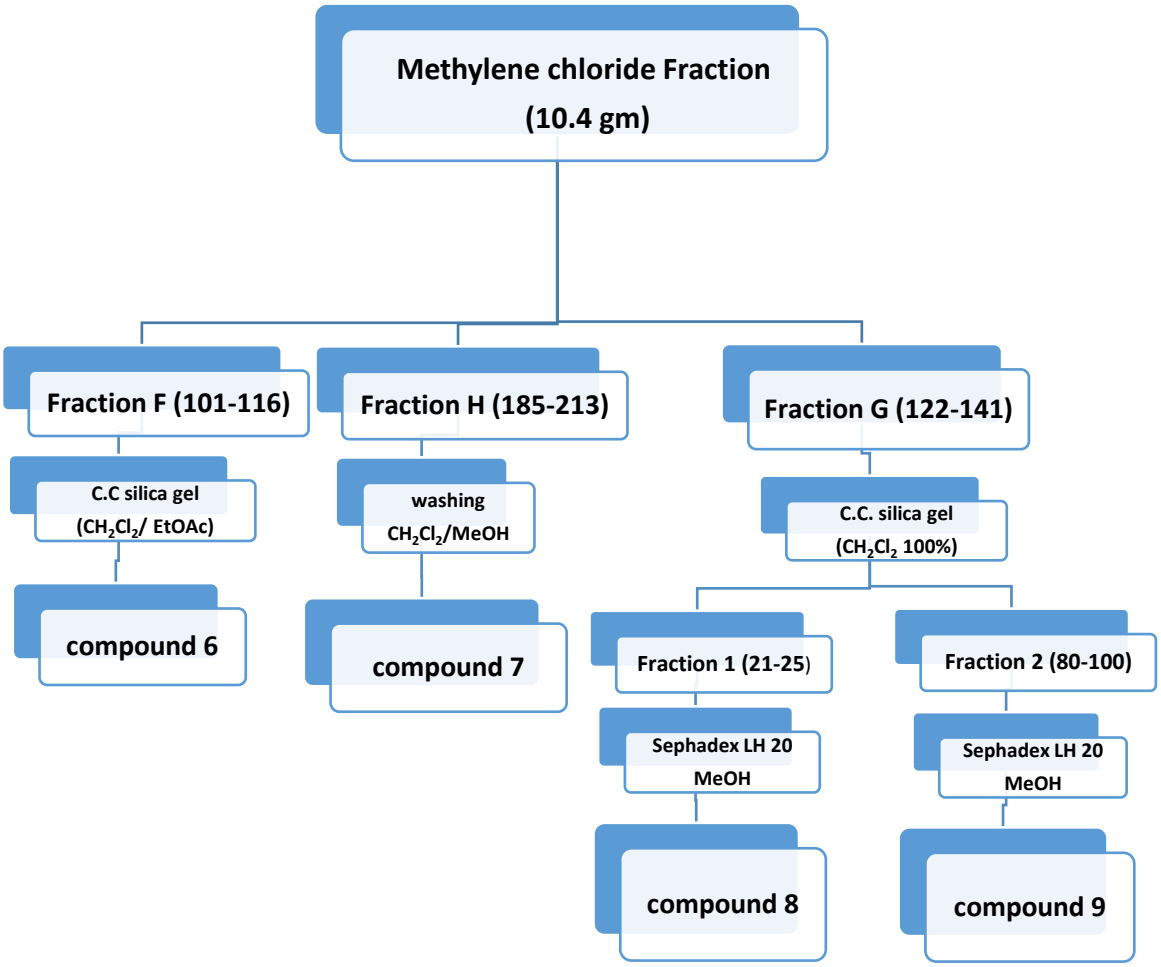

Flowchart 2: Phytochemical investigation of methylene chloride fraction of aerial part of *Lactuca serriola*

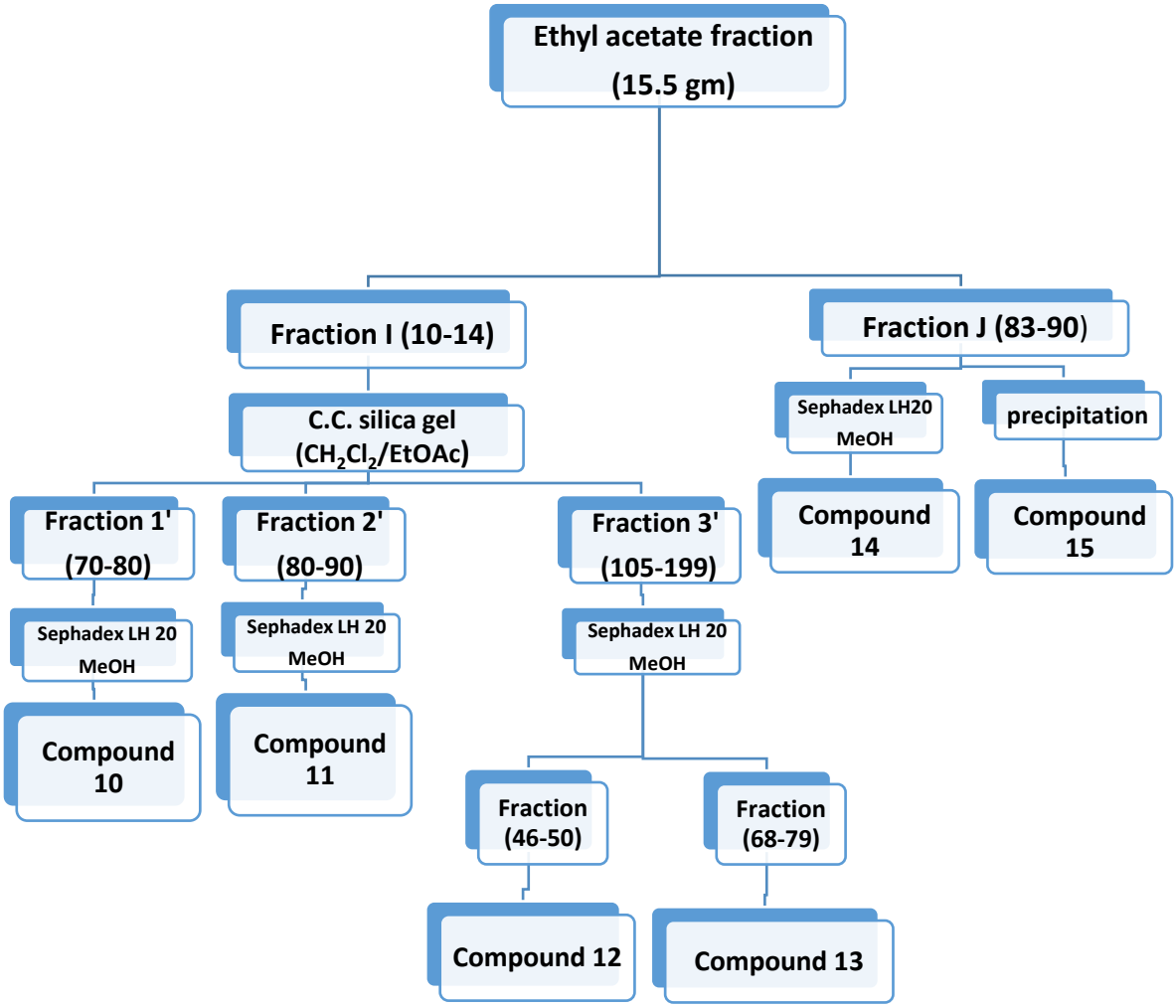

Flowchart 3: Phytochemical investigation of ethyl acetate fraction of aerial part of *Lactuca serriola*

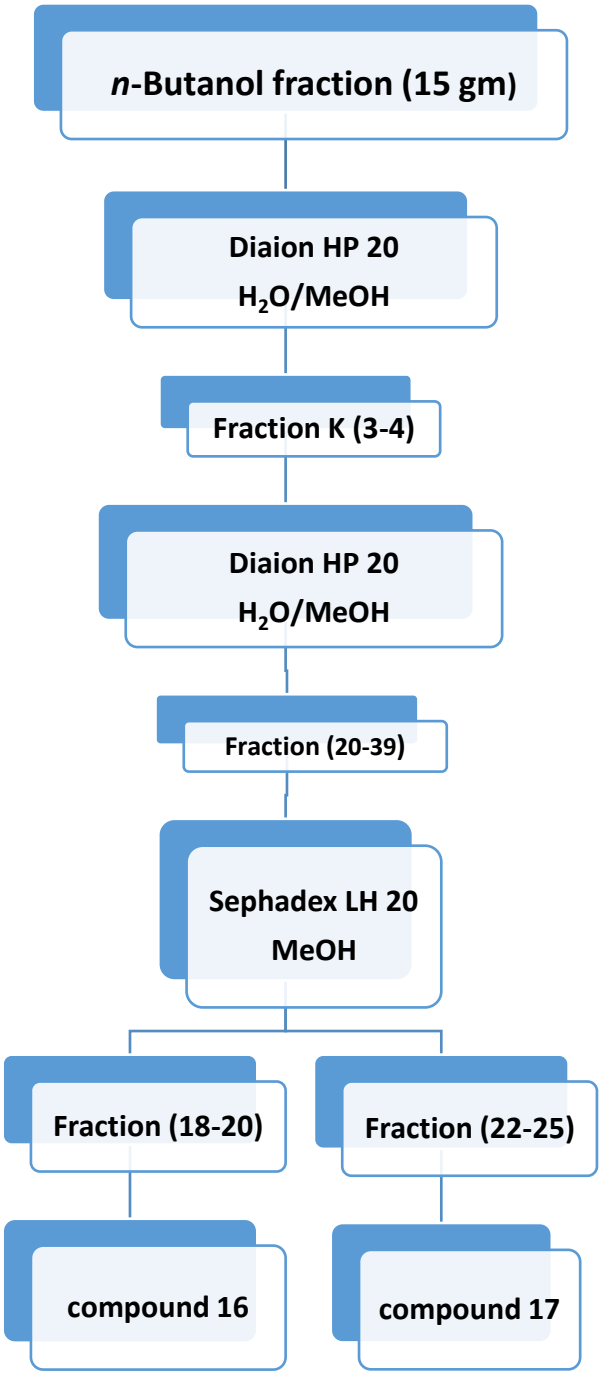

Flowchart 4: Phytochemical investigation of *n*-butanol fraction of aerial part of *Lactuca serriola*

1.3. Biological Activity Assessments

1.3.1. Determination of α-Glucosidase Activity

α-Glucosidase inhibitory activity was carried out according to [1] with minor modifications. In a 96-well plate, reaction mixture containing 10 µL alpha-glucosidase (1 U/mL), 50 µL phosphate buffer (100 mM, pH = 6.8) and 20 µL of varying concentrations of extracts and compounds (1000 to 7.81 µg/mL) was preincubated at 37°C for 15 min. Then, 20 µL P-NPG (5 mM) was added as a substrate and incubated further at 37°C for 20 min. The reaction was stopped by adding 50 µL Na_2CO_3 (0.1 M). The absorbance of the released p-nitrophenol was measured using Multiplate Reader at 405 nm. Acarbose at various concentrations 1000 to 7.81 µg/mL) was used as a standard. Wells without test substance was used as a control and each experiment was performed in triplicates. The results were expressed as percentage inhibition, which was calculated using the formula: **Inhibitory activity (%) = (1 – $A_{test}/A_{control}$) ×100**

1.3.2. Determination of ABTS Radical Scavenging Activity

The assay was carried out according to [2] with minor modifications. The ABTS (2,2′-Azino-bis(3-ethylbenzothiazoline-6-sulfonic acid) radical cation (blue-dark green) was prepared by mixing equal volumes of ABTS stock solution (colorless; 7 mM in distilled H2O) and $K_2S_2O_8$ stock solution (potassium persulfate; 3.5 mM in distilled H2O). The mixture was allowed to stand in the dark at R.T. for 12-16 h until the reaction was complete. The $ABTS^{+\cdot}$ solution was prepared by diluting the $ABTS^{+\cdot}$ stock solution in pure EtOH to have an absorbance ($A_{control}$) of 0.7±0.02 at a wavelength of 734 nm and was equilibrated with an incubator at 30 °C. Free radical scavenging activity was assessed by mixing 1.5 mL of the blue-green $ABTS^{+\cdot}$ solution with 10 µL of the extract/ compound at various concentrations ranging from 10 to 60 µM (in distilled H2O, pure EtOH, or mixture of both of them). The change in absorbance at 734 nm was immediately monitored after 15 min (A_{test}). Ascorbic acid was used as a standared. The decrease in absorbance can represent % inhibition which is calculated as follow: **% inhibition = ($A_{control} – A_{test}$)/ $A_{control}$ X 100**

1.3.3. Determination of DPPH Radical Sscavenging Activity

The DPPH (2,2-diphenyl-1-picryl-hydrazyl-hydrate) free radical assay was carried out according to the method of [3]. 100 µL of freshly prepared DPPH reagent (0.1% in methanol) were added to 100 µL of the sample/ compound at various concentrations (dissolved in DMSO and diluted in methanol) in 96 wells plate **(n=6)**, the reaction was incubated at room temperature for 30 min in dark. At the end of incubation time, the resulting reduction in DPPH color intensity was measured at 540 nm. Trolox was used as a standared. Data are represented as means ± SD according to the following equation: **% inhibition = ($A_{control} – A_{test}$)/ $A_{control}$ X 100**

1.3.4. Determination of Ferric Reducing Antioxidant Power (FRAP)

The ferric reducing ability assay was carried out according to the method of [4] with minor modifications to be carried out in microplates. A freshly prepared TBTZ reagent (300 mM Acetate Buffer (PH=3.6), 10 mM TBTZ in 40 mM HCl, and 20 mM $FeCl_3$, in a ratio of 10:1:1 v/v/v, respectively). 190 µL from the freshly prepared TPTZ reagent were mixed with 10 µL of the extract/compound in 96 wells plate **(n=6)** where compound 10, 11, 14 at 1 mM, compound 12, 13, 15 at 0.166 mM, the MeOH and pet. ether extract at 2 mg/mL and the CH_2Cl_2, EtOAc and *n*-BuOH extract

at 0.333 mg/mL, the reaction was incubated at room temperature for 30 min in dark. At the end of incubation time the resulting blue color was measured at 593 nm. Data are represented as means ± SD. Torolox stock solution of 10 mg/mL in methanol was used as standard at various concentrations from 500 to 7.8 µg/mL.

Compound 1:

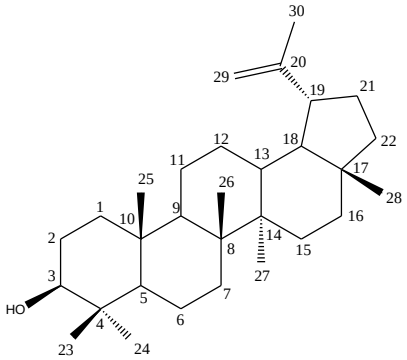

Table S1. ^{1}H (400 MHz) and APT (100 MHz) data of compound **1** in $CDCl_3$.

H/C no.	^{1}H-NMR	APT	^{1}H-NMR* [5]	^{13}C-NMR* [5]
1		38.7		38.1
2		27.4		27.4
3	3.21 (1H, *dd*, *J*= 5.2, 11.2)	79.0	3.21 (*dd*, *J*= 2.0, 6.0 Hz)	79.1
4		38.9		38.7
5		55.3		55.3
6		18.3		18.3
7		34.3		34.3
8		40.8		40.9
9		50.4		50.4
10		37.1		37.2
11		20.9		21.0
12		25.1		25.2
13		38.1		38.9
14		42.8		42.9
15		27.5		27.5
16		35.6		35.6
17		43.0		43.0
18		48.3		48.0
19	2.40 (1H, *m*)	48.0		48.0
20		151.0		151.0
21		29.9		29.9
22		40.0		40.0
23	1.05 (3H, *s*)	28.0	1.00 (s)	28.0
24	0.81 (3H, *s*)	15.4	0.79 (s)	15.4
25	0.85 (3H, *s*)	16.1	0.83 (s)	16.1
26	0.96 (3H, *s*)	16.0	0.95 (s)	16.0
27	0.78 (3H, *s*)	14.6	0.76 (s)	14.6
28	0.99 (3H, *s*)	18.0	0.97 (s)	18.0
29	4.59 (1H, *dd*, *J*=2.4, 1.6)	109.3	4.57 (s)	109.3
	4.71 (1H, *d*, *J*=2.4)		4.68 (s)	
30	1.70 (3H, *s*)	19.3	1.68 (s)	19.3

* ^{13}C-NMR (50 MHz), ^{1}H-NMR (200 MHz) is measured in $CDCl_3$

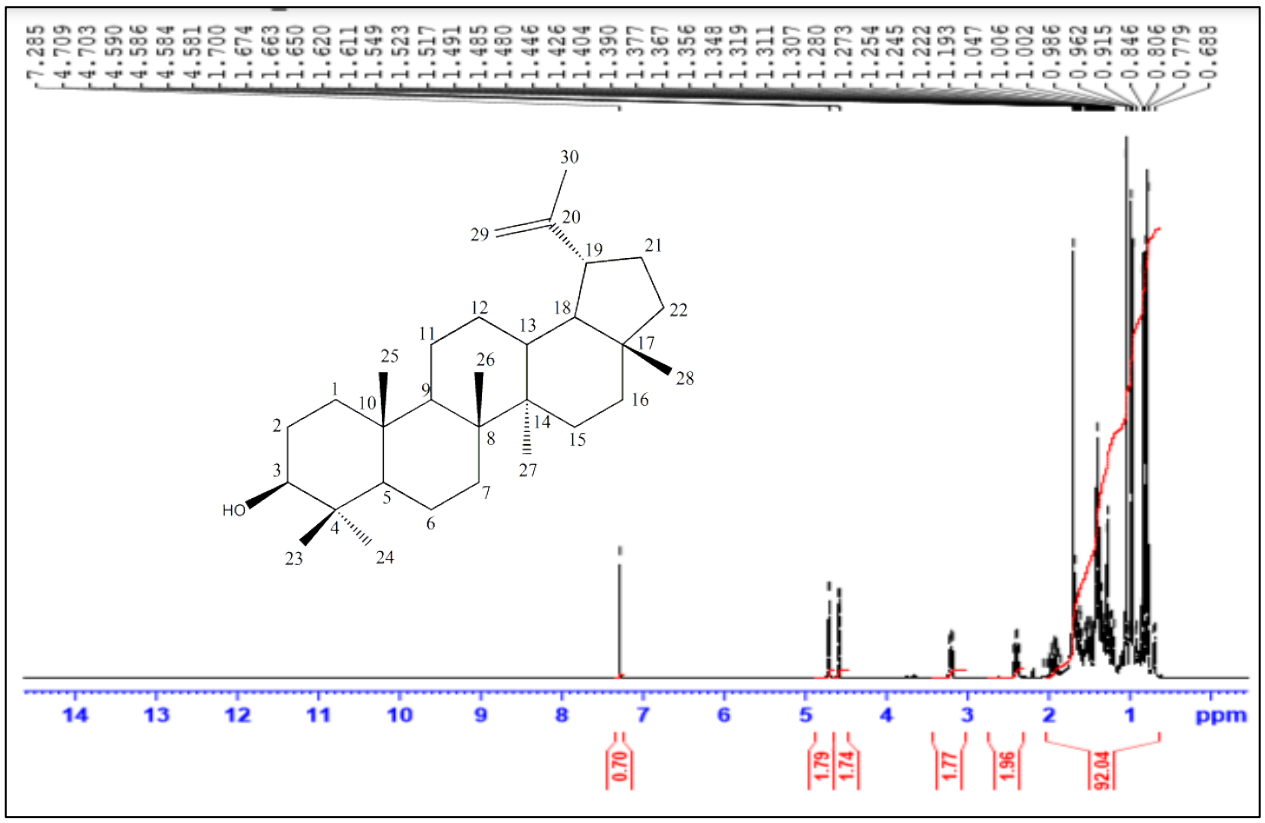

Figure S1: ^{1}H (400 MHz) data of compound **1** in $CDCl_3$

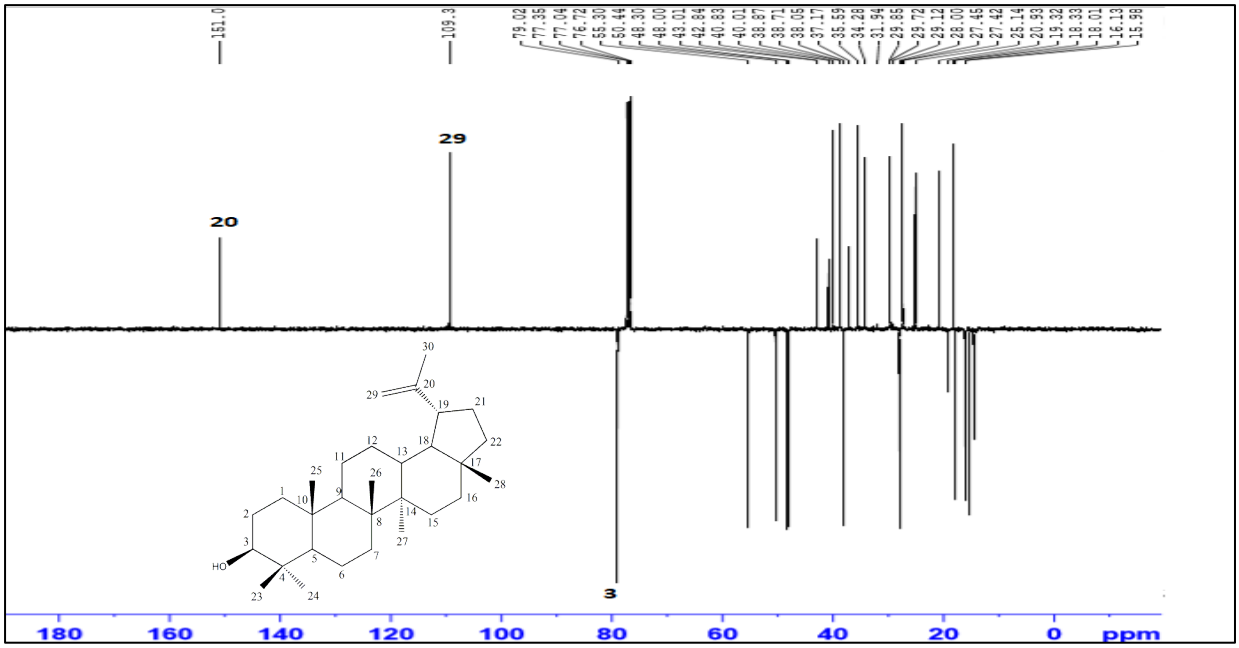

Figure S2: APT (100 MHz) data of compound **1** in $CDCl_3$

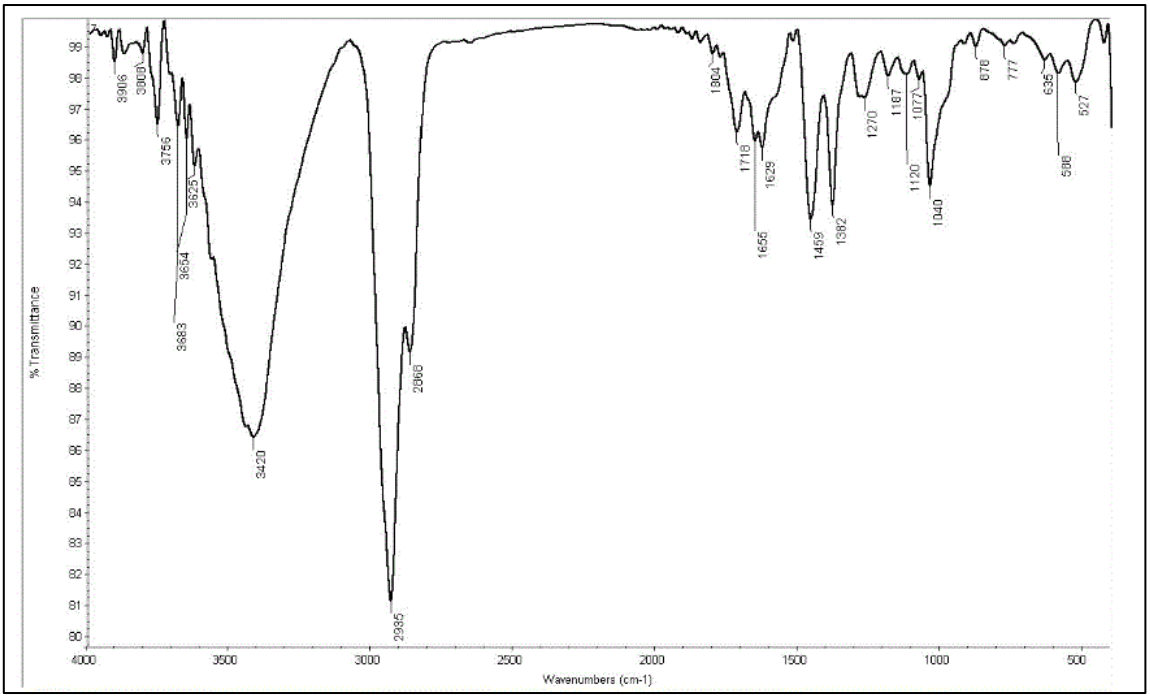

Figure S3: IR spectrum of compound **1** (KBr)

Compound 2:

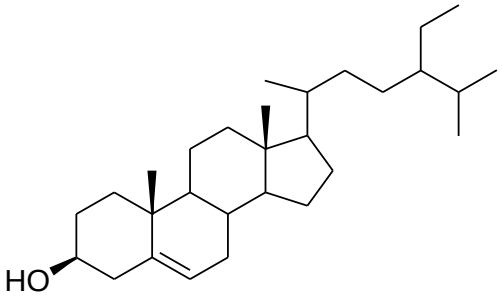

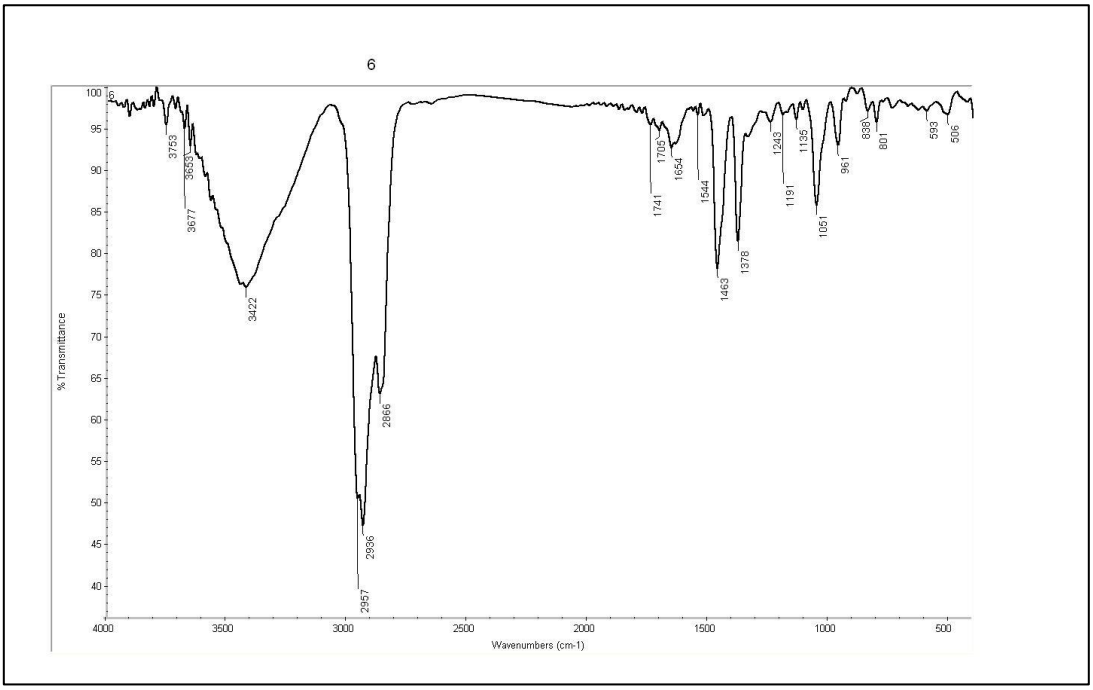

Figure S4: IR spectrum of compound **2** (KBr)

Compound 3:

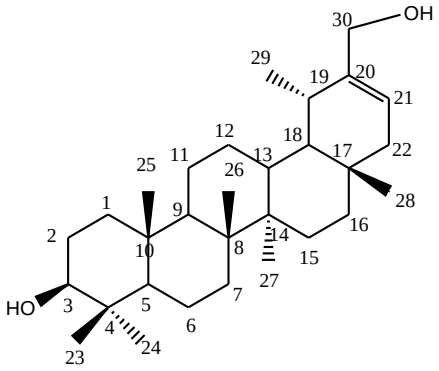

Table S2: ^{1}H (400 MHz) and APT (100 MHz) data of compound **3** in $CDCl_3$

H/C no.	^{1}H-NMR	APT	^{13}C-NMR [6]
1		39.3	38.7
2		28.1	27.6
3	3.19 (1H, *dd*, *J*=11.2, 5.2)	79.6	79.0
4		39.4	38.9
5		55.8	55.3
6		18.9	18.3
7		34.7	34.3
8		41.6	41.1
9		50.9	50.4
10		37.2	37.1
11		22.1	21.6
12		27.9	27.0
13		39.7	39.2
14		42.9	42.4
15		27.5	27.4
16		37.6	36.7
17		34.2	34.5
18		48.9	48.5
19	2.30 (1H, *t*, *J*=7.6)	32.5	32.0
20		144.2	143.7
21	5.56 (H, *d*, *J*=6.4)	121.3	120.7
22		42.2	42.2
23	0.74 (3H, *s*)	15.3	15.4
24	0.95 (3H, *s*)	28.5	28.0
25	0.85 (3H, *s*)	16.8	16.3
26	1.01 (3H, *s*)	16.6	16.0
27	0.94 (3H, *s*)	14.7	14.8
28	0.83 (3H, *s*)	18.3	17.7
29	0.99 (3H, *d*, *J*= 6.4)	23.1	22.5
30	4.12 (1H, *d*, *J*=13.2)	66.0	65.5
	4.01 (1H, *d*, *J*=12.4)		

*^{13}C-NMR is measured in $CDCl_3$ at 100 MHz

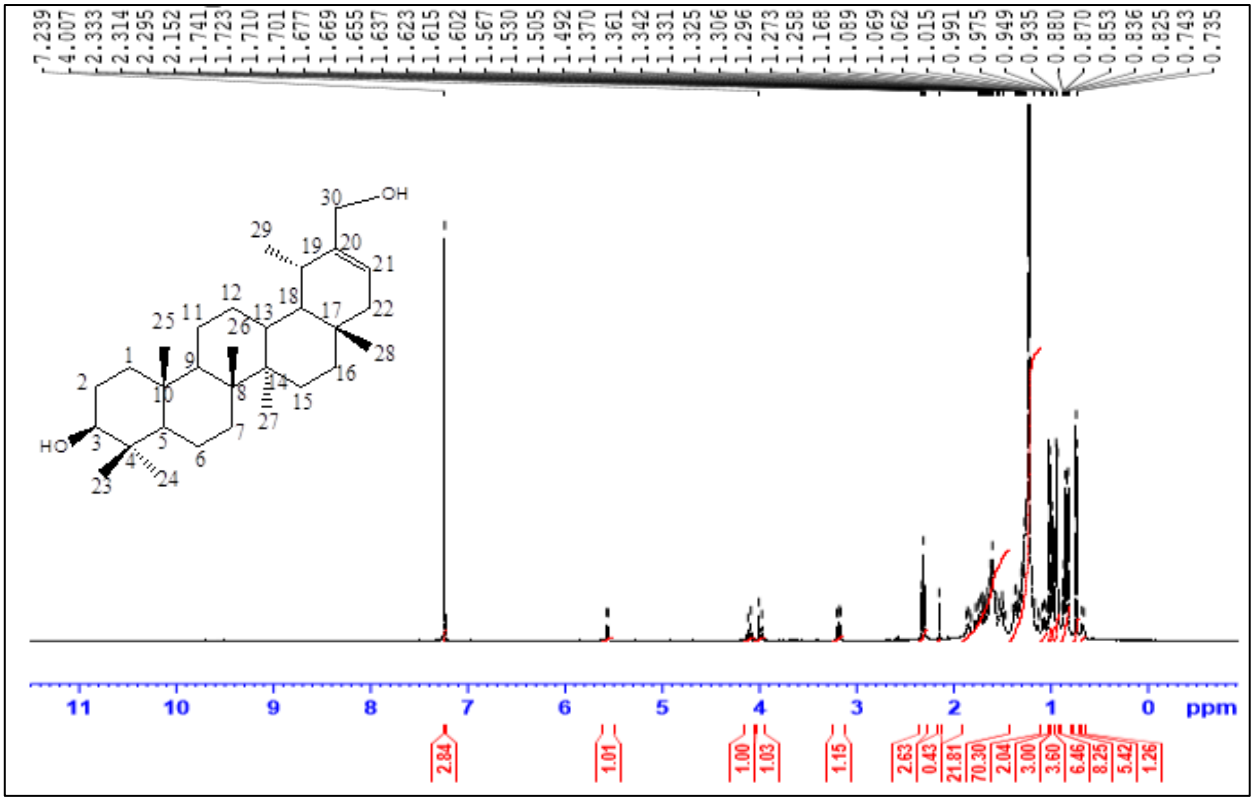

Figure S5: ^{1}H (400 MHz) data of compound **3** in $CDCl_3$

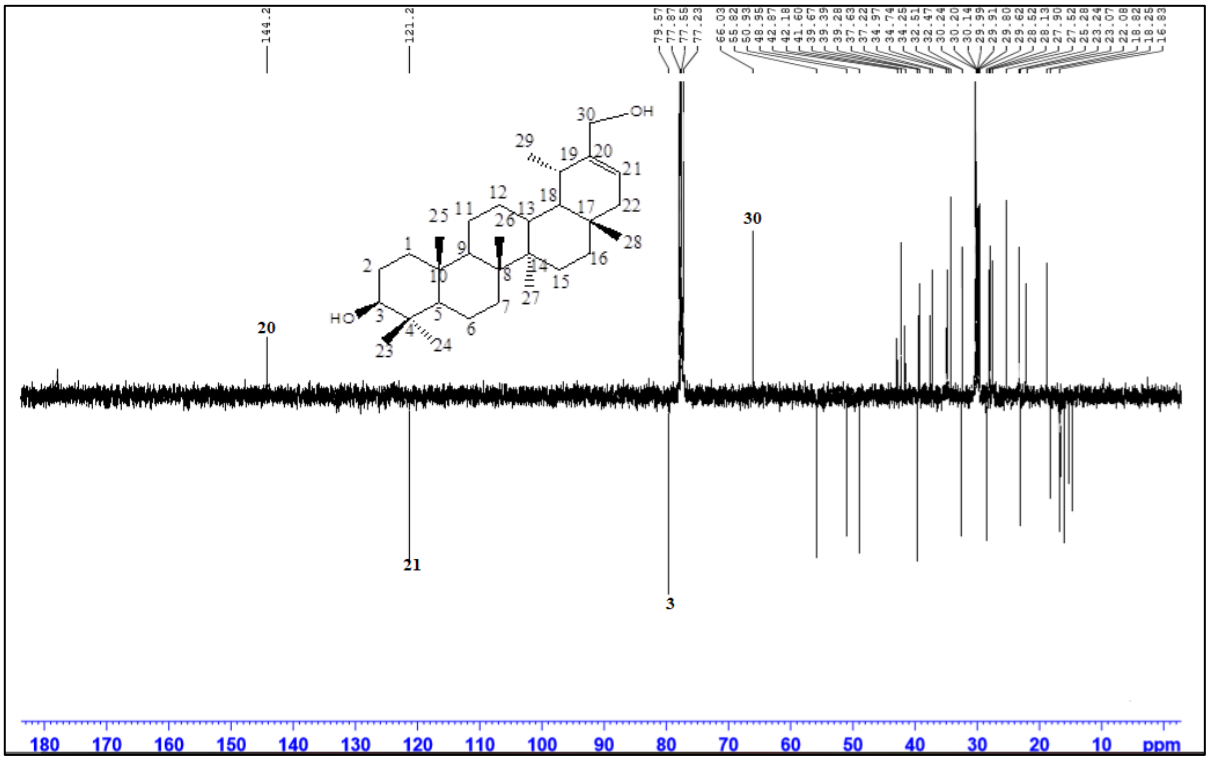

Figure S6: APT (100 MHz) data of compound **3** in $CDCl_3$

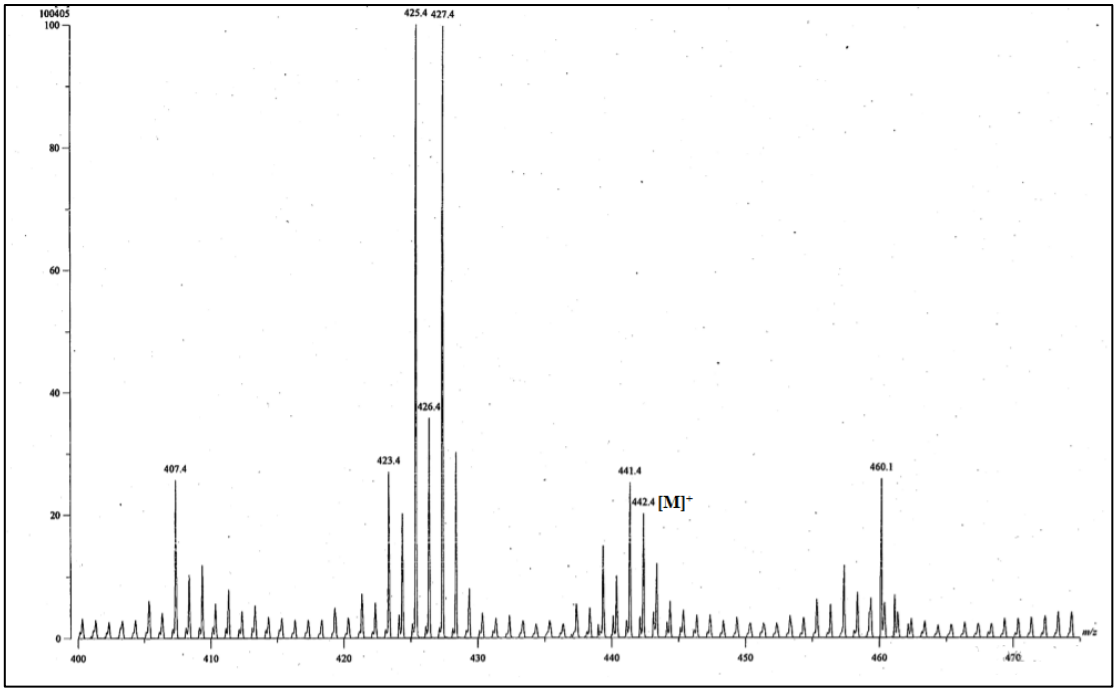

Figure S7: HR-FAB-MS of compound 3

Compound 4:

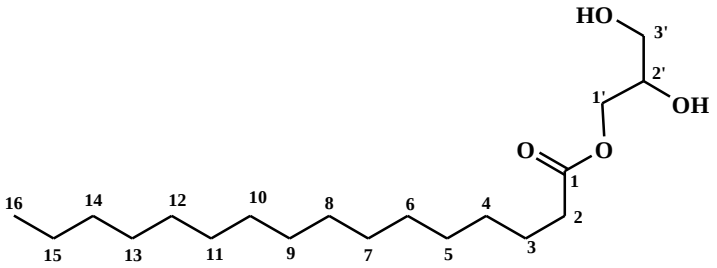

Table S3: ^{1}H (600 MHz) and APT (150 MHz) data of compound **4** in $CDCl_3$, CD_3OD mixture

H/C no.	^{1}H-NMR	APT	^{1}H-NMR* [7]	^{13}C-NMR* [7]
1		175.7		
2	2.35 (2H, *t*, *J*=7.8)	35.1	2.34 (3H, *t*)	34.2
3	1.62 (2H, *m*)	26.1	1.62 (2H, *m*)	24.6
4-13	1.28 (26H, *m*)	30.2-30.8	1.24-1.28 (28H, *m*)	29.1-29.7
14		33.1		29.1-29.7
15		23.8		29.1-29.7
16	0.89 (3H, *t*, *J*= 7.2)	14.6	0.87 (3H, *t*)	14.1
1'	4.08 (1H, *dd*, *J*= 11.4, 6.0)	64.1	4.13 (1H, *dd*)	63.3
	4.16 (1H, *dd*, *J*= 11.4, 4.8)		4.19 (1H, *dd*)	
2'	3.83 (1H, *m*)	71.2	3.92 (1H, *dd*)	70.3
3'	3.56 (1H, *t*, *J*=4.8)	66.6	3.59 (1H, *dd*)	65.2
	3.67 (1H, *dd*, *J*=10.8, 4.8)		3.69 (1H, *dd*)	

* ^{13}C and ^{1}H-NMR are measured in $CDCl_3$

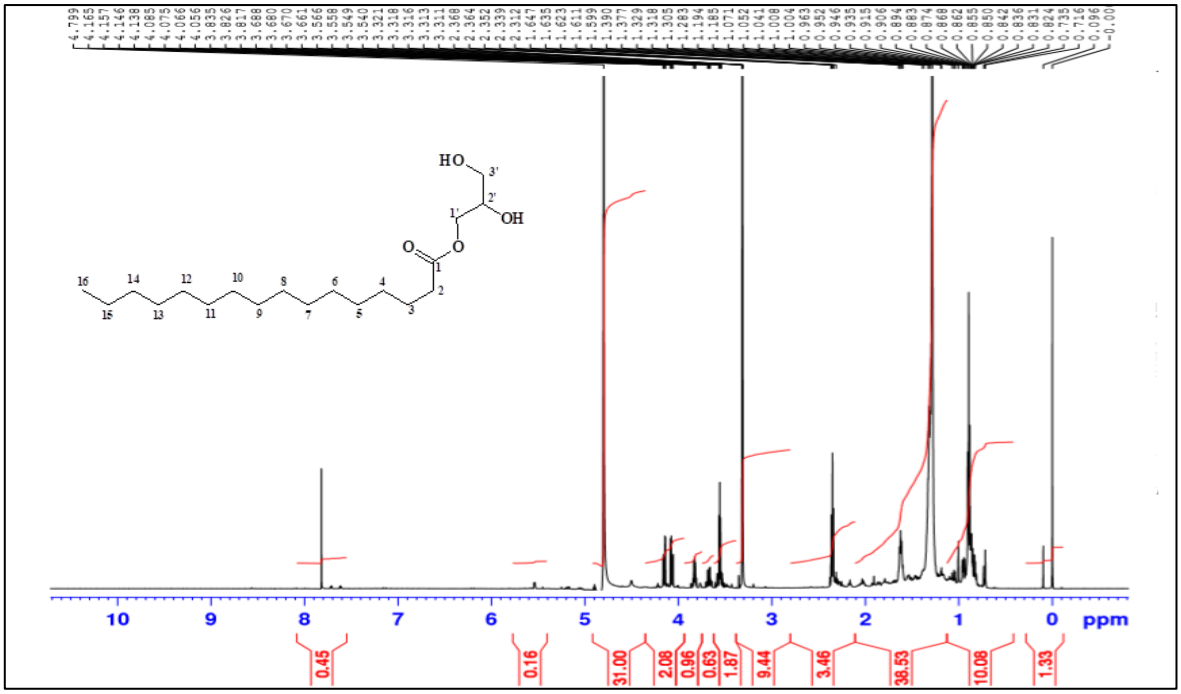

Figure S8: ^{1}H (600 MHz) data of compound **4** in $CDCl_3$, CD_3OD mixture

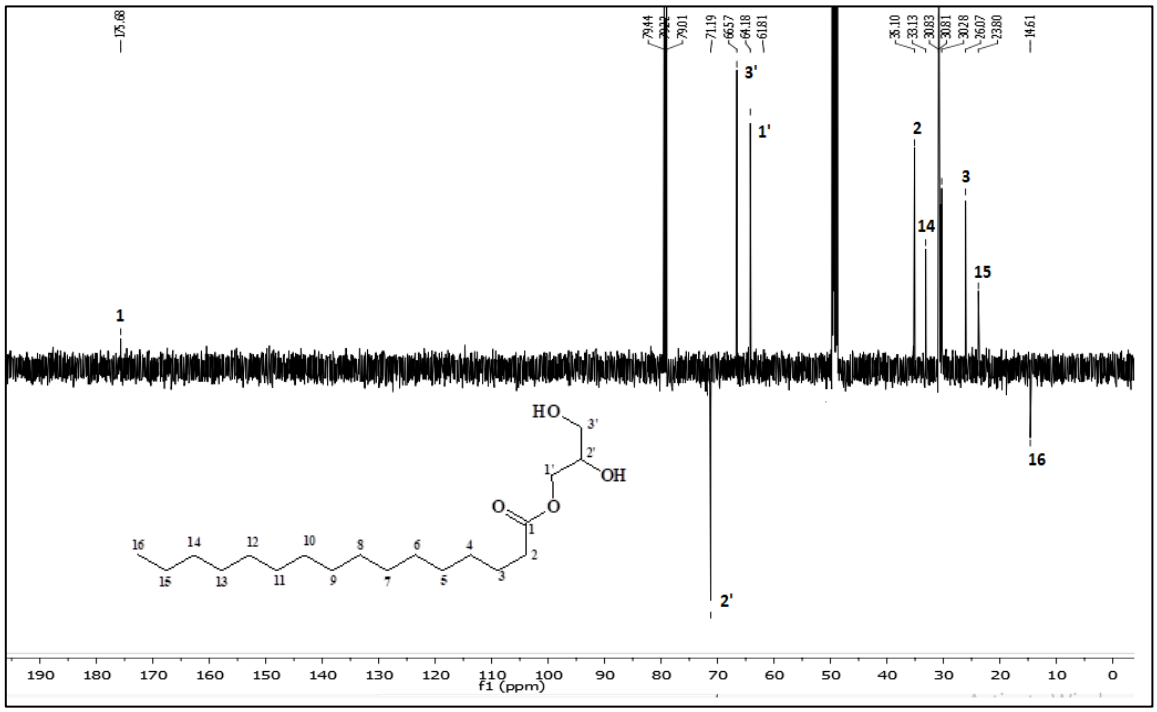

Figure S9: ^{13}C NMR (APT, 150 MHz) data of compound **4** in $CDCl_3$, CD_3OD mixture

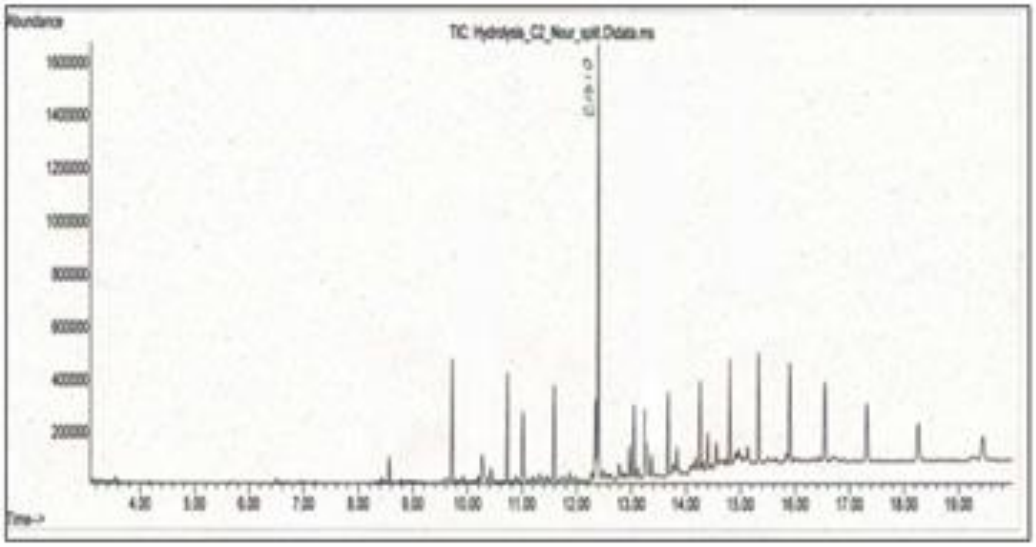

Figure S10: GC-MS of fatty acid methyl ester of compound **4**

Compound 5:

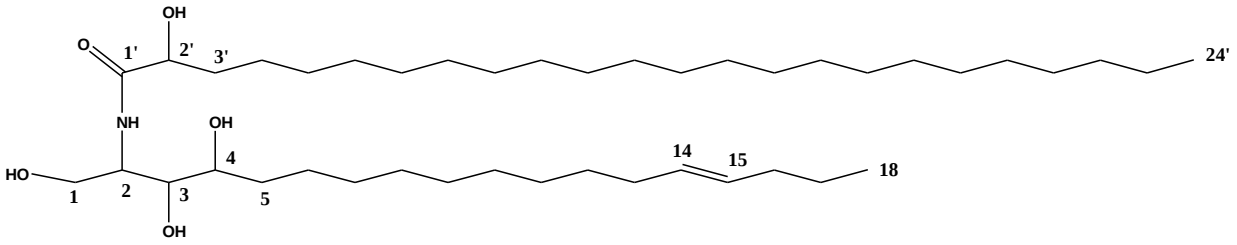

Table S4: ^{1}H (600 MHz) and APT (150MHz) data of compound **5** in $CDCl_3$

H/C no.	^{1}H-NMR	APT	^{13}C-NMR* [8]
1	1a 3.74 (1H, *dd*, *J*= 12.0, 4.8) 1b 3.81 (1H, *dd*, *J*= 12.0, 4.2)	61.0	61.3
2	4.09 (1H, *m*)	51.5	51.8
3	3.53 (1H, *m*)	75.6	72.4
4	3.54 (1H, *m*)	72.3	72.2
5	5a 1.41(1H, *m*) 5b 1.71 (1H, *m*)	32.5	34.7
6	1.58 (1H, *m*)	25.8	25.4
7-12	1.26- 1.31	29.1-29.6	29.5-32.1
13	1.97 (2H, *m*)	32.5	33.1
14	5.40 (2H, t, *J*=5.4)	129.8	130.0
15	5.40 (2H, t, *J*=5.4)	130.8	132.1
16	1.97 (2H, *m*)	32.5	32.8
17	1.29	22.6	26.1
18	0.88 (6H, t, *J*= 6.6)	13.9	14.2
1'	…….	175.7	176.1
2'	4.04 (1H, *dd*, *J*= 8.4, 3.6)	72.2	75.5
3'	1.80 (1H, *m*) 1.58 (1H, *m*)	34.3	32.8
4'	1.41 (1H, *m*)	25.2	22.9
5'-23'	1.26- 1.31	29.1-31.8	29.5-32.1
24'	0.88 (6H, t, *J*= 6.6)	13.9	14.2

*^{13}C-NMR is measured in $CDCl_3$ at 100 MHz.

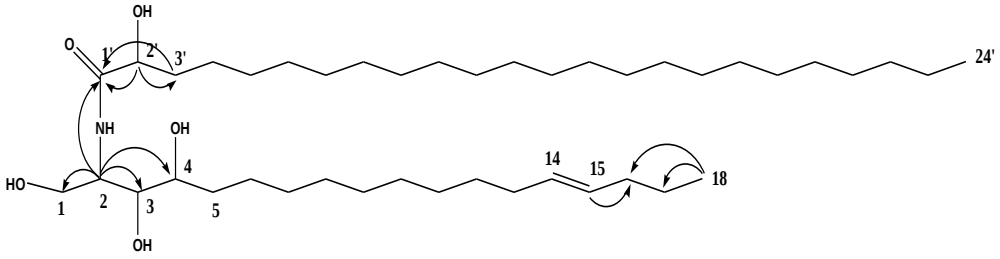

Figure S11: Selected HMBC correlations of compound **5**

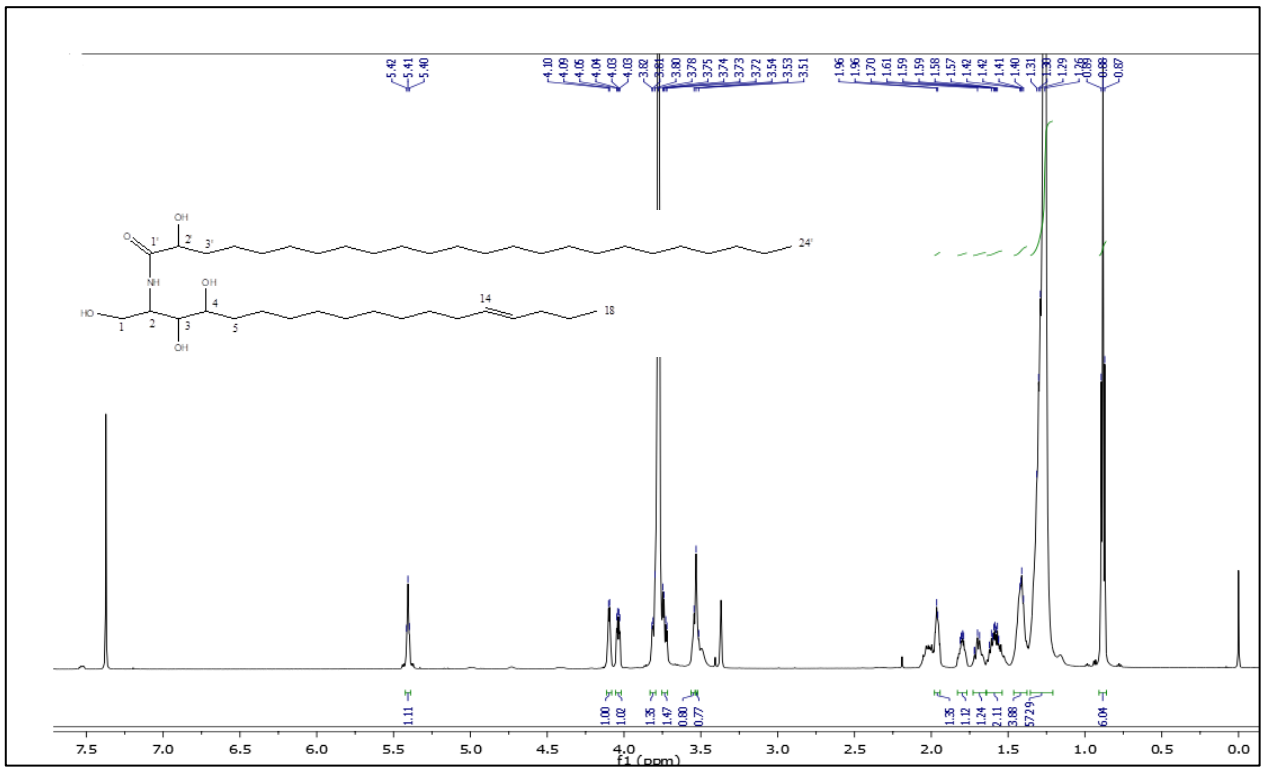

Figure S12: ^{1}H (600 MHz) data of compound **5** in $CDCl_3$

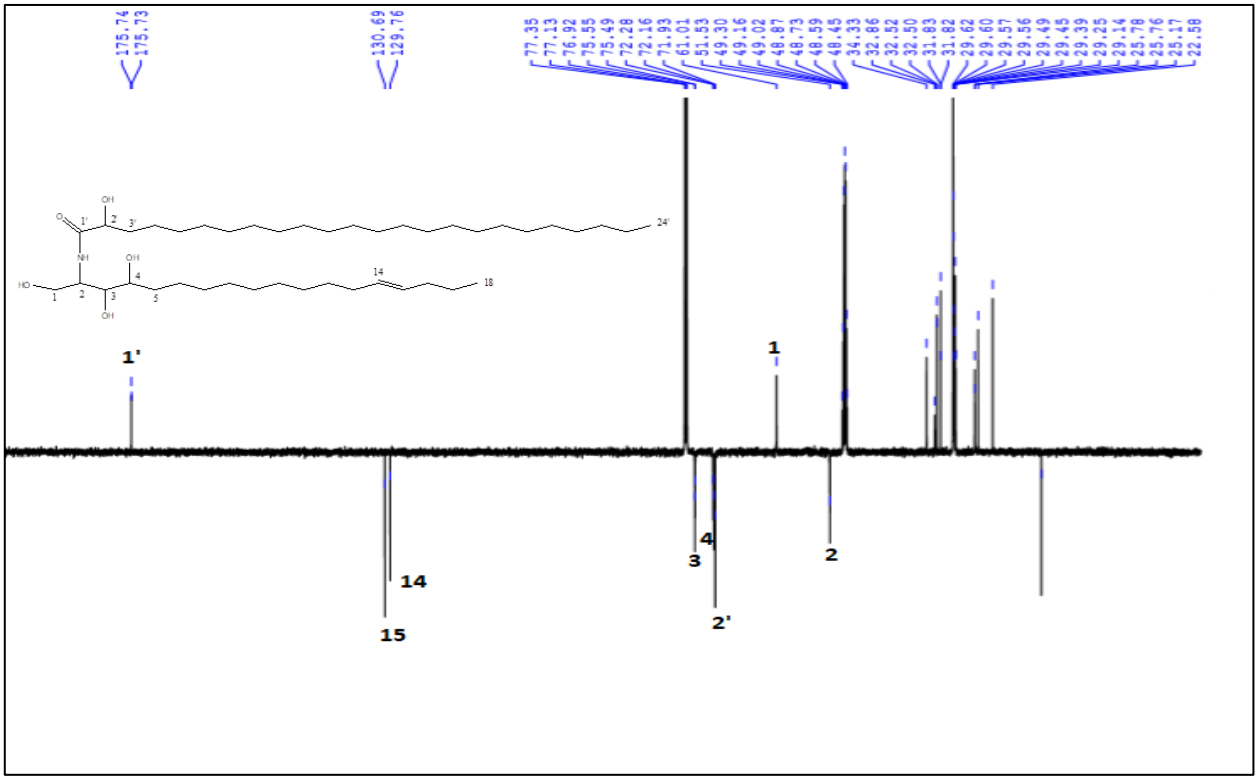

Figure S13: APT (150MHz) data of compound **5** in $CDCl_3$

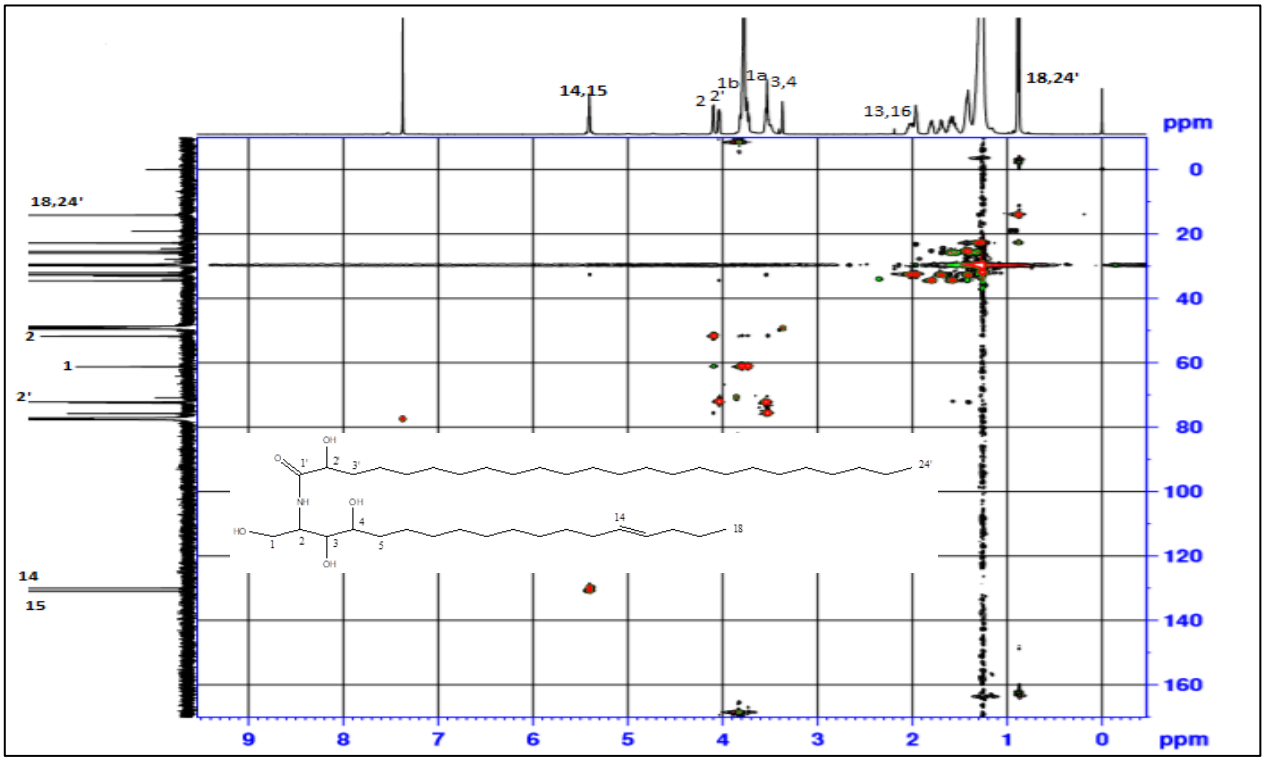

Figure S14: HSQC experiment of compound **5** in $CDCl_3$

×

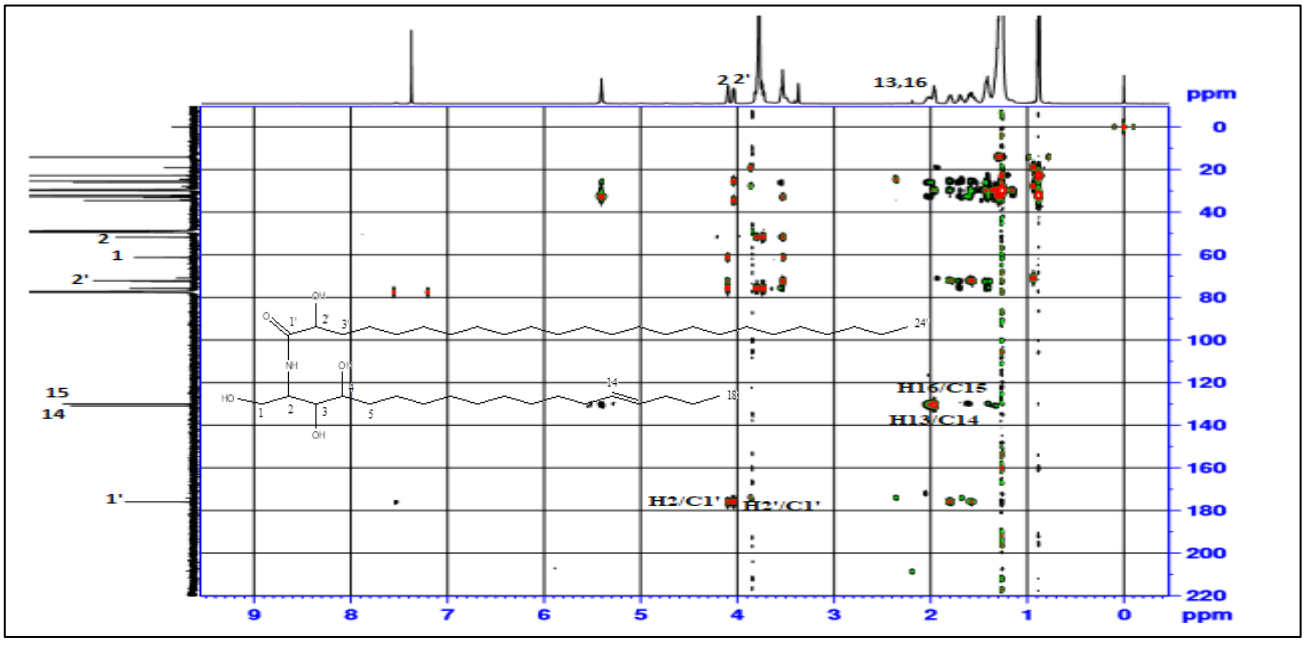

Figure S15: HMBC experiment of compound **5** in $CDCl_3$

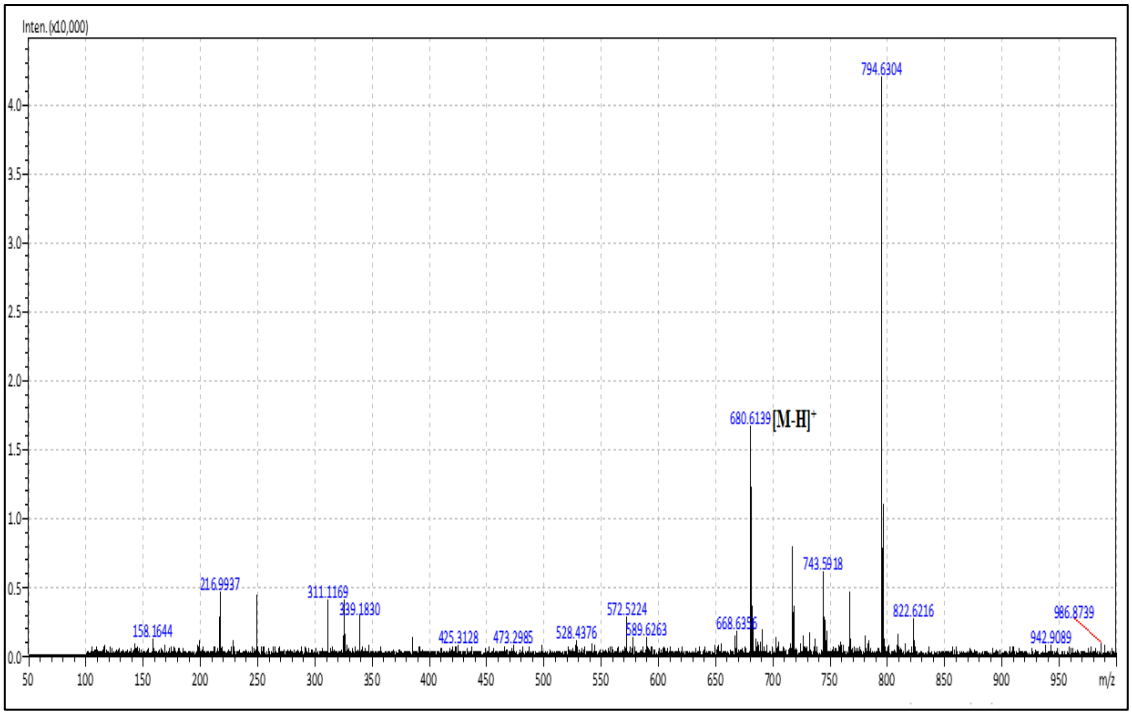

Figure S16: Negative HR-ESI-TOF-MS spectrum of compound **5**

Compound 6

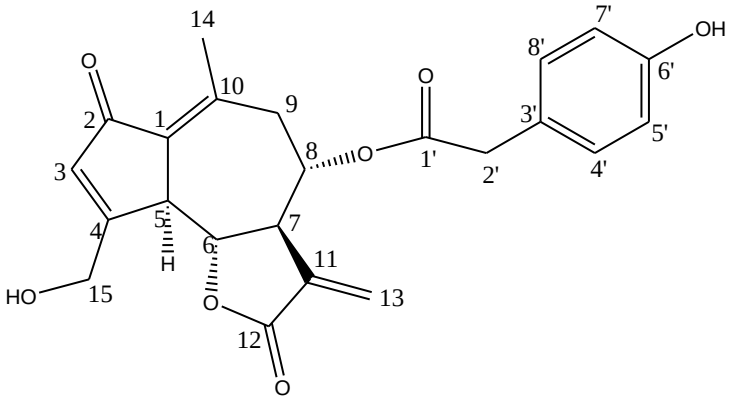

Table S5: ^{1}H (500 MHz) and ^{13}C NMR (125MHz) data of compound **6** in C_5D_5N

H/C no.	^{1}H-NMR	^{13}C-NMR	^{1}H-NMR*[9]	^{13}C-NMR*[9]
1		133.8		133.0
2		194.7		194.1
3	6.97 (1H, *d*, *J*=1)	133.3	6.32 (*d*, *J*=1.08)	132.0
4		175.2		174.8
5	3.80 (1H, *d*, *J*=10.5)	48.7	3.89 (*d*, *J*=10.80)	47.5
6	3.71 (1H, *t*, *J*=10.5)	81.2	3.96 (*t*, *J*= 10.80)	80.3
7	3.46 (1H, *tt*, *J*=10.0, 3.0)	54.5	3.52 (*tt*, *J*=10, 2.60)	52.9
8	5.04 (1H, *dt*, *J*=10.5, 1.5)	69.9	4.88 (*dt*, *J*=10.50, 1.90)	69.2
9	2.79 (1H, *t*, *J*= 13.0) 2.44 (1H, *dd*, *J*=13.0, 2.2)	44.0	2.87 (*dd*, *J*=13.30, 10) 2.30 (*dd*, *J*=13.30, 2)	43.4
10		144.9		144.6
11		137.1		136.5
12		168.5		168.1
13	5.51 (1H, *d*, *J*=3.0) 6.15 (1H, *d*, *J*=3.0)	121.3	5.90 (*d*, *J*=3.20) 5.38 (*d*, *J*=3.00)	120.9
14	2.46 (3H, *s*)	20.9	2.08 (*s*)	20.6
15	4.72 (H,*d*, *J*= 18.5) 5.28 (H, *d*, *J*=18.5)	62.4	4.70 (*ddd*, *J*=18.80, 5.80, 1.90) 4.29 (*ddd*, *J*=19.10, 5.60, 1.50)	61.3
1'		171.2		170.7
2'	3.83 (2H)[a]	40.8	3.70 (*d*, 15.50) 3.66 (*d*, 15.50)	39.7
3'		124.5		123.8
4'	7.39 (2H)[a]	131.1	7.11 (*dd*, *J*=6.60, 1.50)	130.4
5'	7.20 (2H, *d*, *J*=6, 1.5)	116.5	6.74 (*dd*, *J*=6.60, 1.50)	115.3
6'		158.3		156.4
7'	7.20 (2H, *d*, *J*=6.0, 1.5)	116.5	6.74 (*dd*, *J*=6.60, 1.50)	115.3
8'	7.39 (2H)[a]	131.1	7.11 (*dd*, *J*=6.60, 1.50)	130.4

[a] Peaks *J* values cannot be determined due to peaks deformity.

*^{13}C and ^{1}H-NMR are measured in DMSO-d_6 at 100 and 400 MHz respectively.

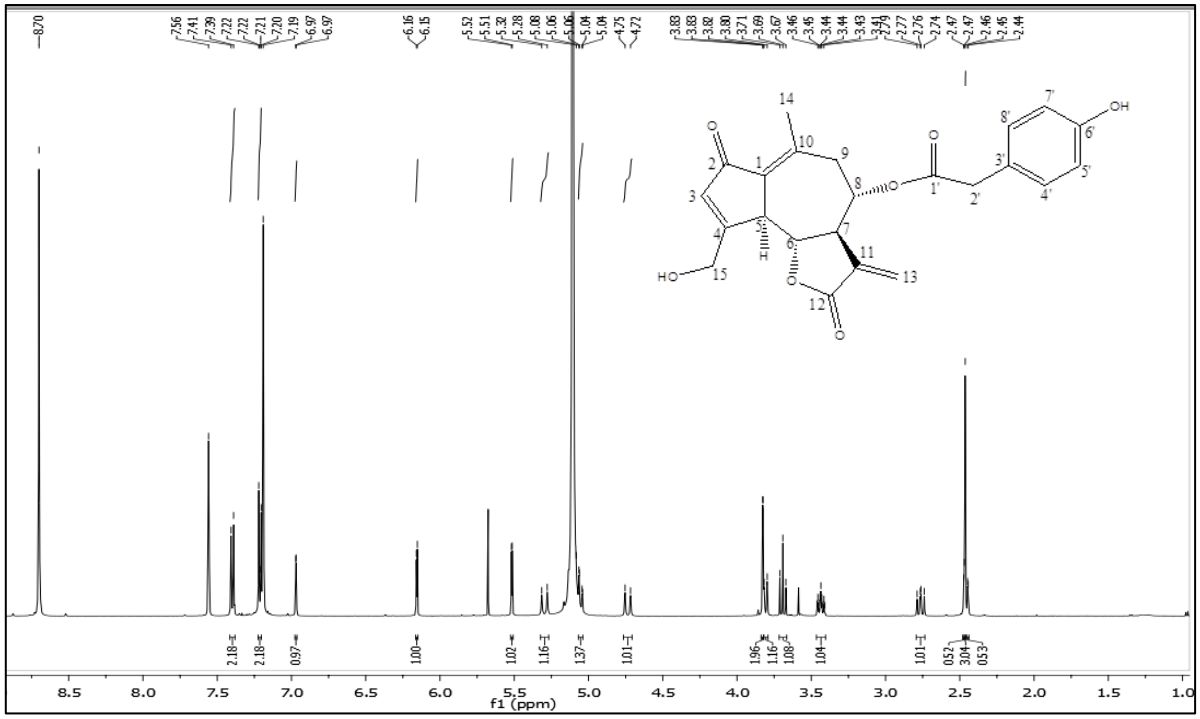

Figure S17: ^{1}H (500 MHz) data of compound **6** in C_5D_5N

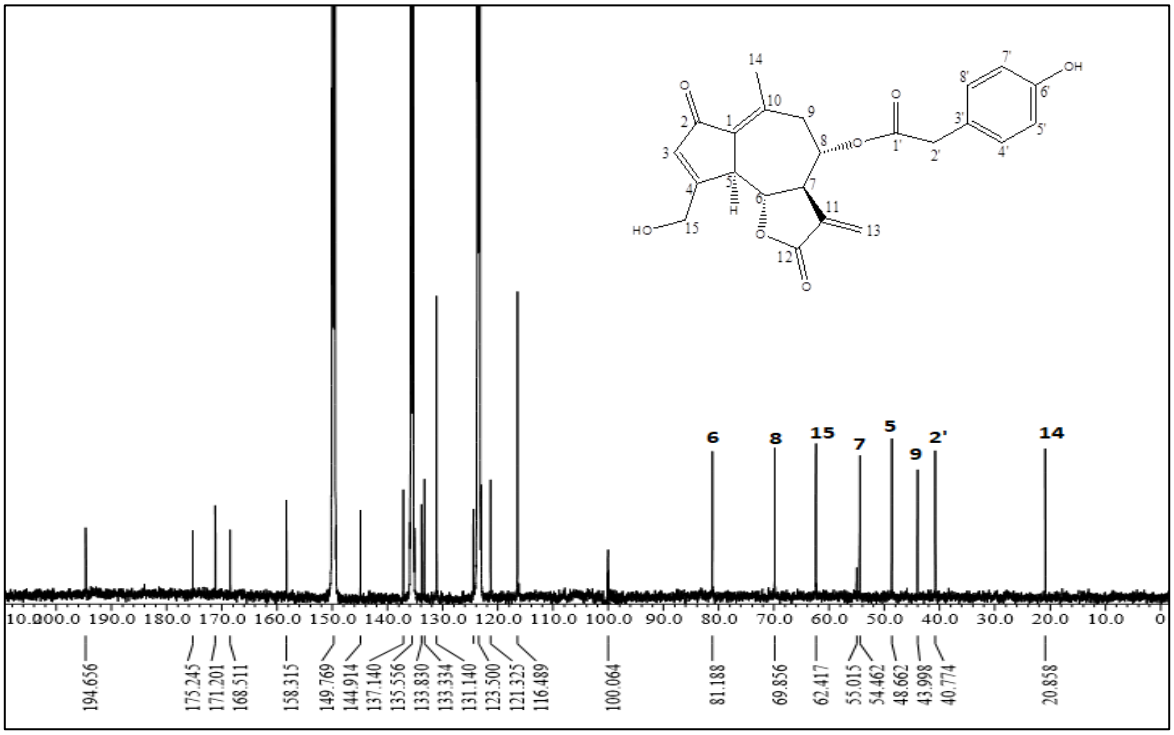

Figure S18: ^{13}C NMR (125MHz) data of compound **6** in C_5D_5N

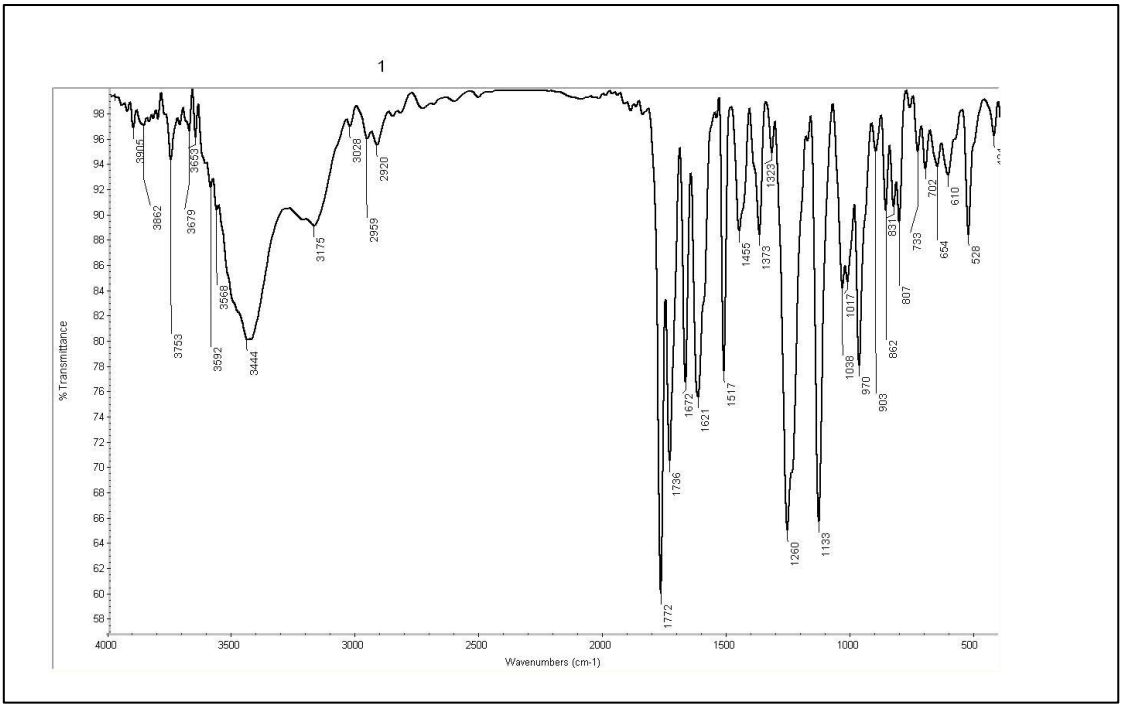

Figure S19: IR spectrum of compound **6** (KBr)

Compound 7:

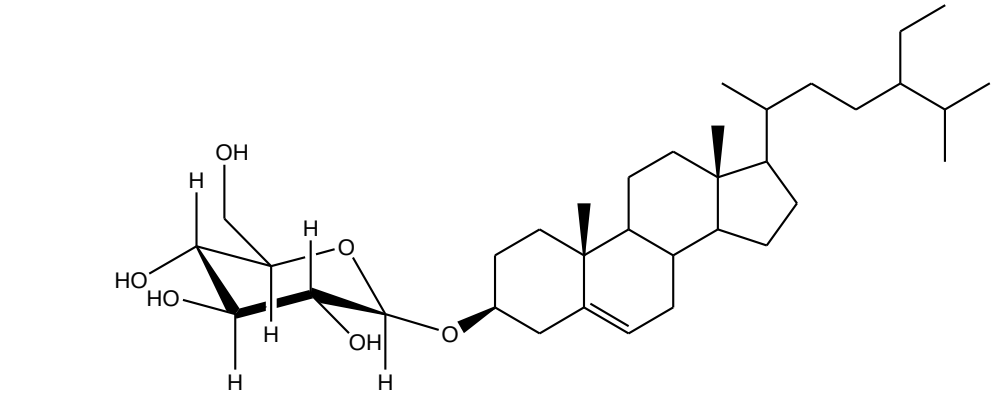

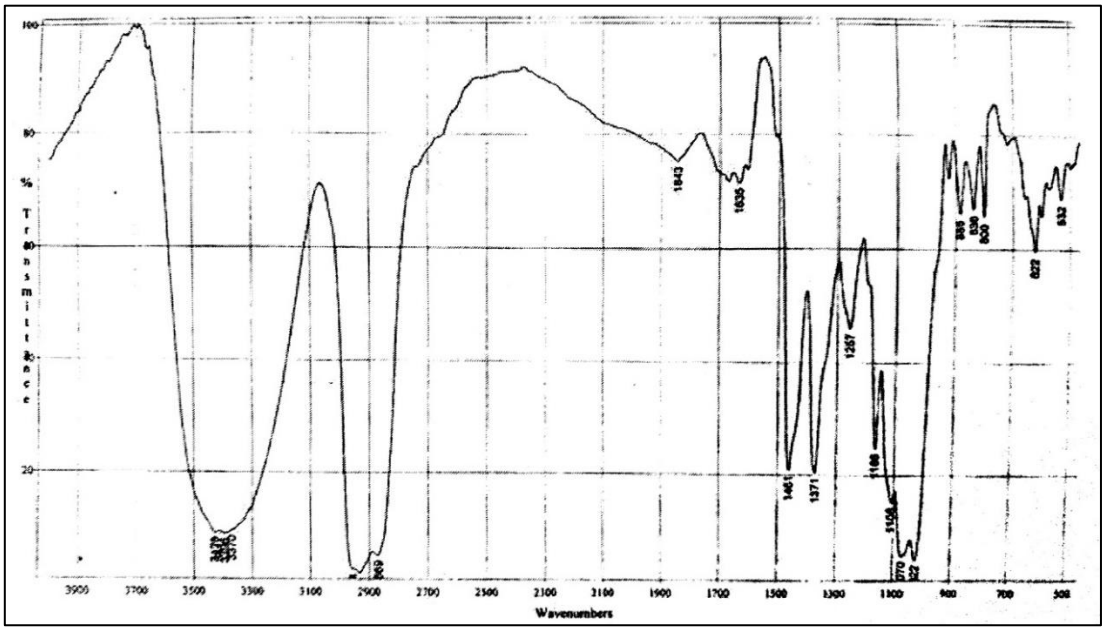

Figure S20: IR spectrum of compound **7** (KBr)

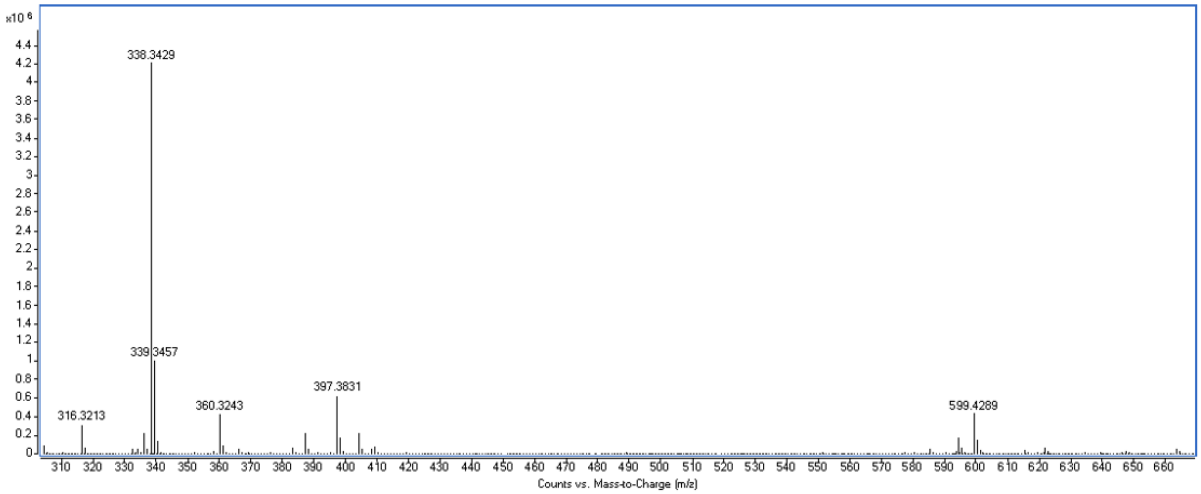

Figure S21 : QTOF-HR-ESI-MS analysis of compound **7** (positive mode)

Compound 8:

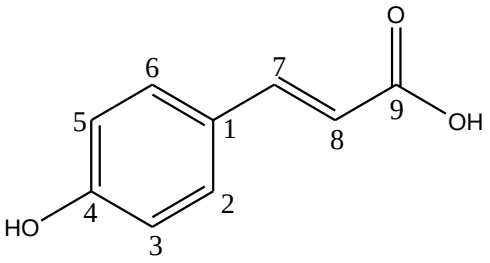

Table S6: ^{1}H (500 MHz) and ^{13}C NMR (125MHz) data of compound **8** in CD_3OD

H/C no.	^{1}H-NMR	^{13}C-NMR	^{1}H-NMR* [10]	^{13}C-NMR *[10]
1	……	127.6		127.3
2	7.41 (2H, *d*, *J*= 8.5)	130.8	7.44 (2H, *d*, *J* = 8.6)	131.1
3	6.78 (2H, *d*, *J*= 8.5)	116.7	6.79 (2H, *d*, *J* = 8.6)	116.8
4	……	160.8		161.2
5	6.78 (2H, *d*, *J*= 8.5)	116.7	6.79 (2H, *d*, *J* = 8.6)	116.8
6	7.41 (2H, *d*, *J*= 8.5)	130.8	7.44 (2H, *d*, *J* = 8.6)	131.8
7	7.51 (1H, *d*, *J*= 16.0)	145.2	7.58 (1H, *d*, *J* = 15.9)	146.5
8	6.27 (1H, *d*, *J*= 16.0)	116.0	6.28 (1H, *d*, *J* = 15.9)	115.8
9		ND		ND

*^{1}H and ^{13}C-NMR are measured in CD_3OD at 500 and 125 MHz respectively.
ND:Not detected .

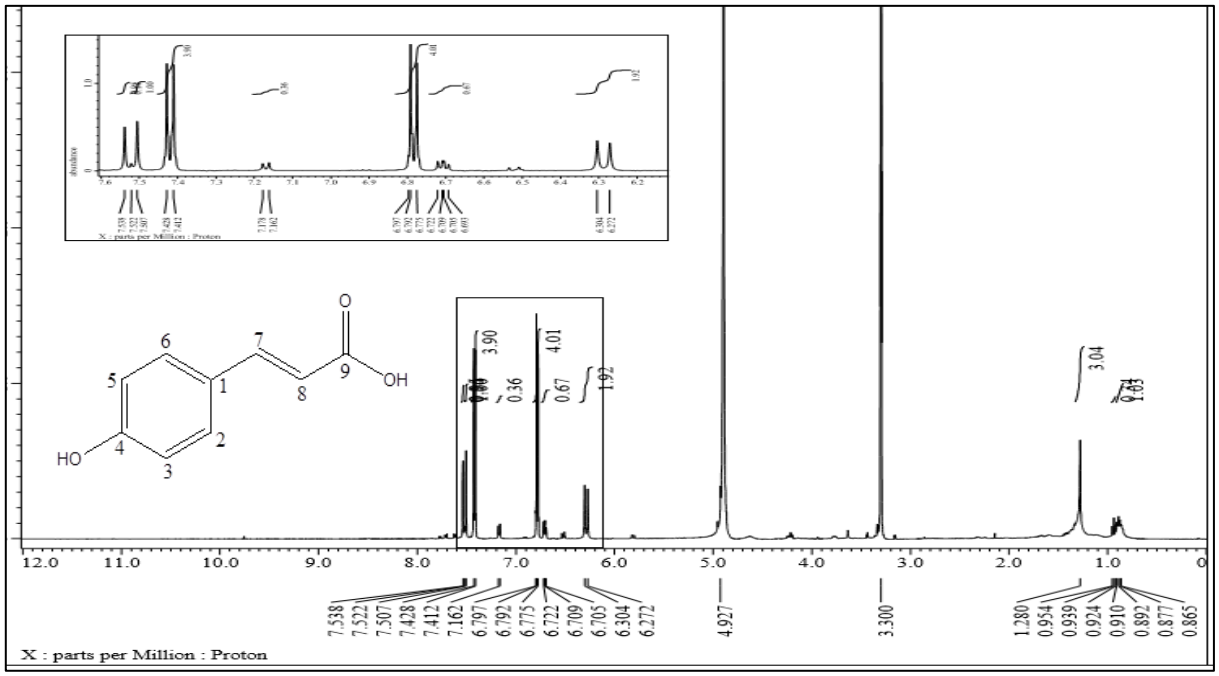

Figure S22: ^{1}H (500 MHz) data of compound **8** in CD_3OD

Figure S23: ^{13}C NMR (125MHz) data of compound **8** in CD_3OD

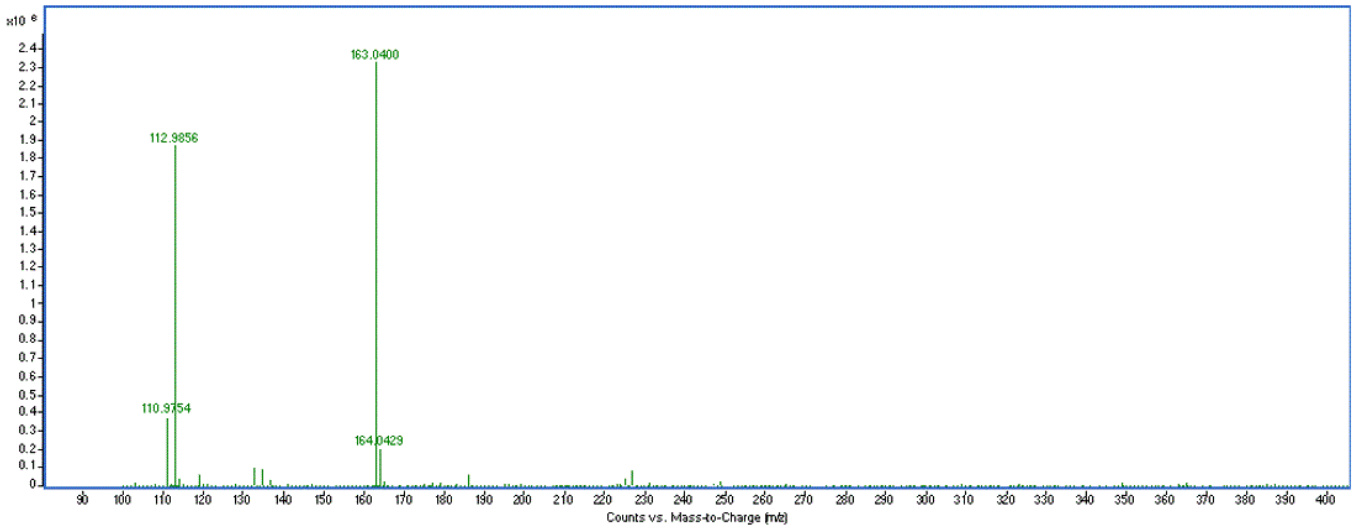

Figure S24: QTOF-HR-ESI-MS analysis (negative mode) of compound **8**

Compound 9:

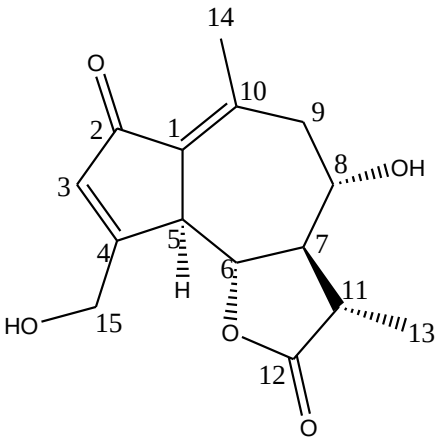

Table S7: ^{1}H (500 MHz) and ^{13}C NMR (125MHz) data of compound **9** in CD_3OD

H/C no.	^{1}H-NMR	^{13}C-NMR	^{1}H-NMR*[11]	^{13}C-NMR* [11]
1		133.1		132.3
2		197.3		195.8
3	6.39 (1H, *d*, *J*=1.0)	133.6	6.44 (br. *s*)	133.1
4		176.5		173.4
5	3.71 (*d*, *J*=9.0)	49.7	3.56 (*d*, *J*=10)	49.2
6	3.67 (*dd*, *J*=10, 1.5)	82.4	3.66 (*dd*, *J*=10,10)	81.2
7	2.15 [a]	62.2	2.15 (*ddd*, *J*=12, 10, 9.6)	61.4
8	3.69 [a]	69.9	3.74 (*m*)	68.0
9	2.40 (*dd*, *J*=14.0, 2.0)	50.0	2.40 (*dd*, *J*=13.6, 2)	49.3
	2.79 (*dd*, *J*=14.0, 11.0)		2.76 (*dd*, *J*=13.6, 10.8)	
10		149.9		148.3
11	2.63 (*q*, *J*=7.0)	42.5	2.59 (*dq*, *J*=12, 7.2)	41.7
12		179.9		178.6
13	1.36 (*d*, *J*=7.0)	15.8	1.43 (*d*, *J*=7.2)	15.3
14	2.41 (*s*)	21.8	2.45 (br. *s*)	21.8
15	4.41 (*dd*, *J*=18.5, 1.0)	63.1	4.43 (*d*, *J*=17.6)	62.2
	4.82 (*dd*, *J*=18.5, 1.0)		4.48 (*d*, *J*=17.6)	

[a] Peaks multiplicity is not clear due to overlapping with other peaks.

*^{1}H and ^{13}C -NMR are measured in $CDCl_3$ at 400 and 100 MHz respectively

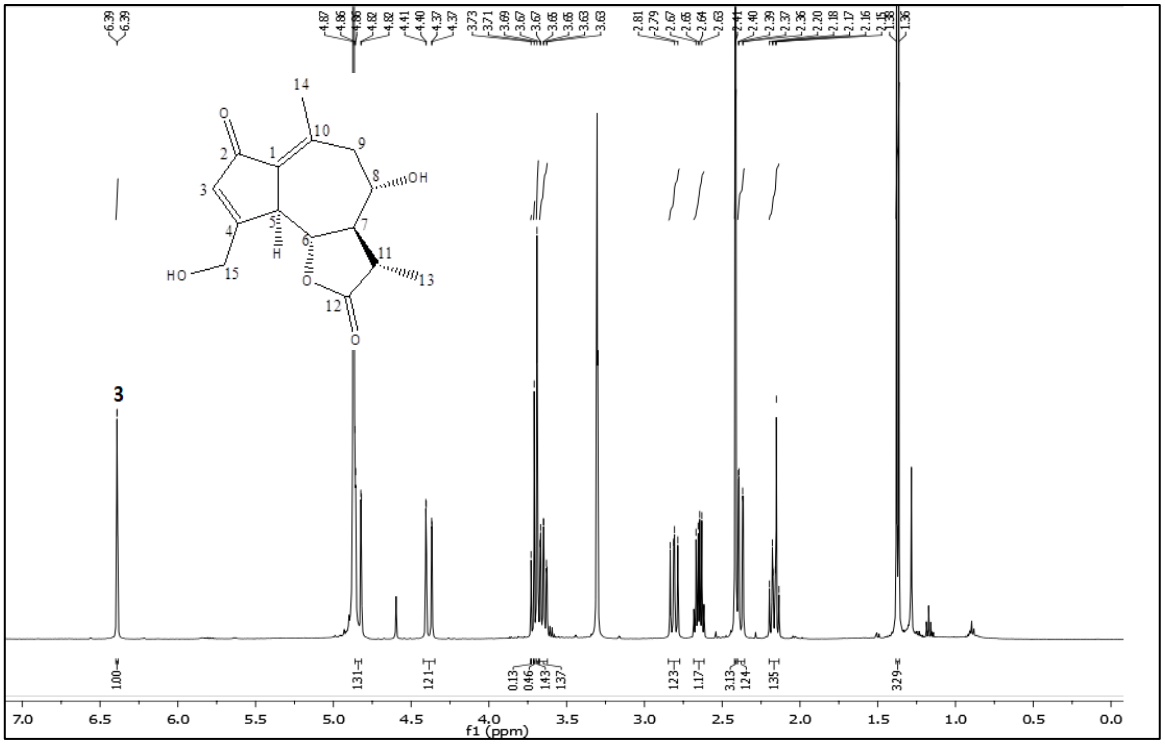

Figure S25: ^{1}H (500 MHz) data of compound **9** in CD_3OD

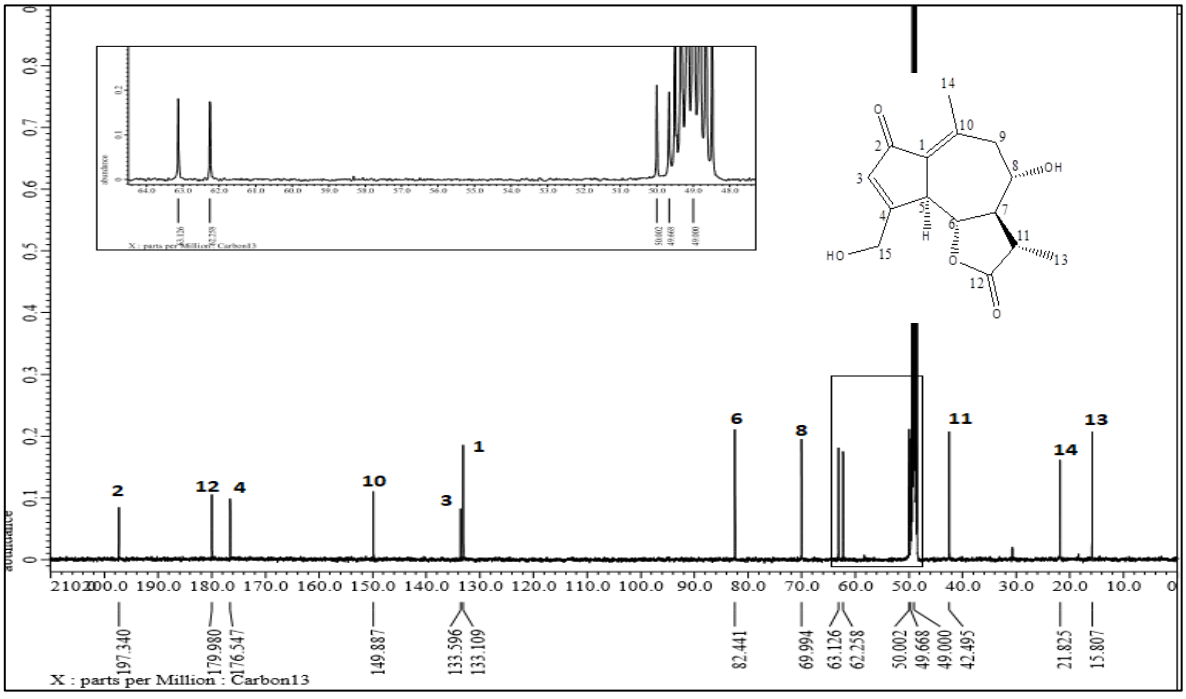

Figure S26: ^{13}C NMR (125 MHz) data of compound **9** in CD_3OD

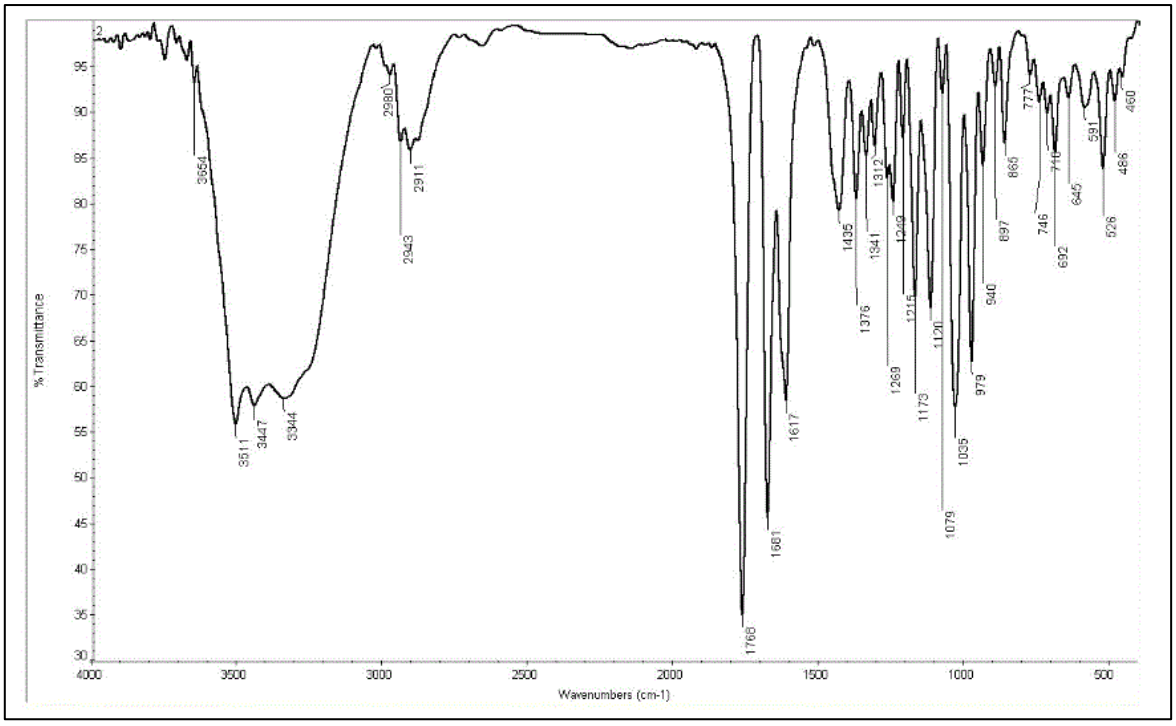

Figure S27: IR spectrum of compound **9** (KBr)

Compound 10:

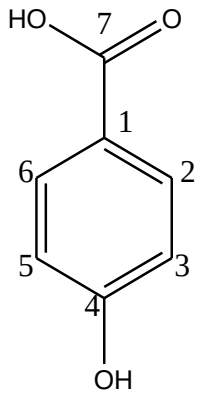

Table S8: ^{1}H (400 MHz) and ^{13}C NMR (100MHz) data of compound **10** in CD_3OD

H/C no.	**^{1}H-NMR**	**^{13}C-NMR**	**^{1}H-NMR*** [10]	**^{13}C-NMR***[10]
1		123.8		122.7
2	7.12 (2H, *d*, *J*=8.4)	130.0	7.87 (2H, *d*, *J* = 8.8 Hz)	133.0
3	6.76 (2H, *d*, *J*=8.0)	114.8	6.80 (2H, *d*, *J* = 8.8 Hz)	116.0
4		156.0		163.4
5	6.76 (2H, *d*, *J*=8.0)	114.8	6.80 (2H, *d*, *J* = 8.8 Hz)	116.0
6	7.12 (2H, *d*, *J*=8.4)	130.0	7.87 (2H, *d*, *J* = 8.8 Hz)	133.0
7		ND		ND

*^{1}H and ^{13}C-NMR are measured in CD_3OD at 500 and 125 MHz respectively.
ND:Not detected .

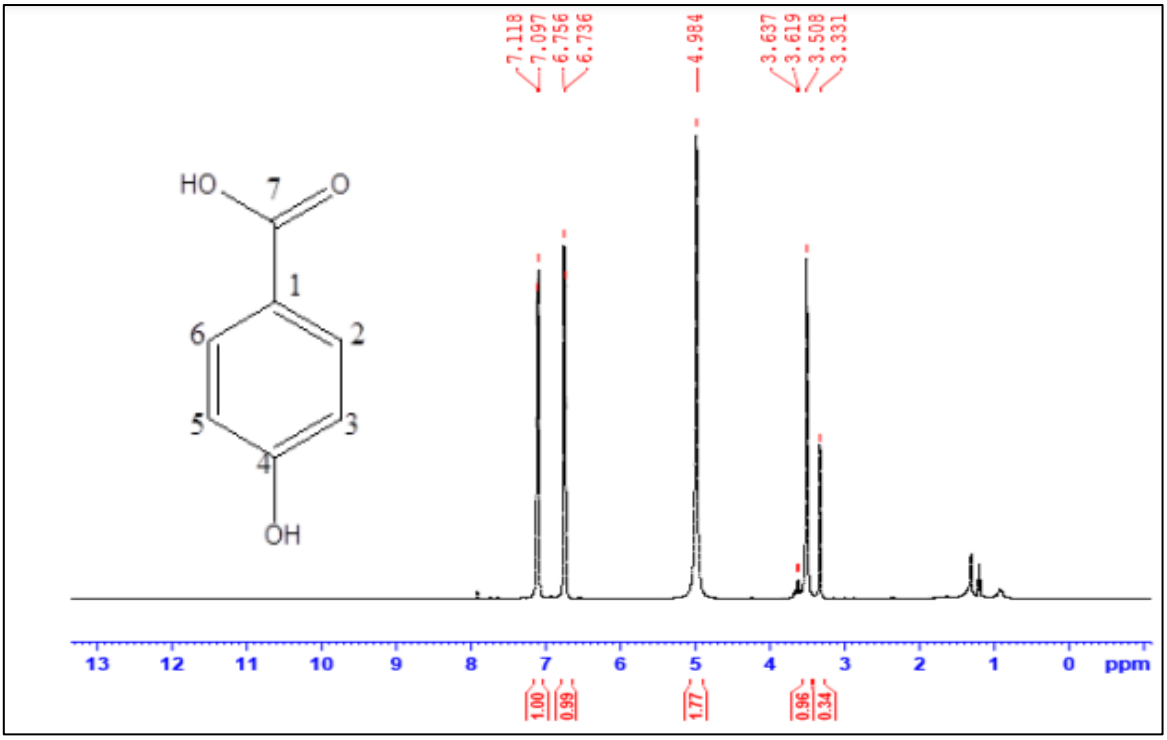

Figure S28: ^{1}H (400 MHz) data of compound **10** in CD_3OD

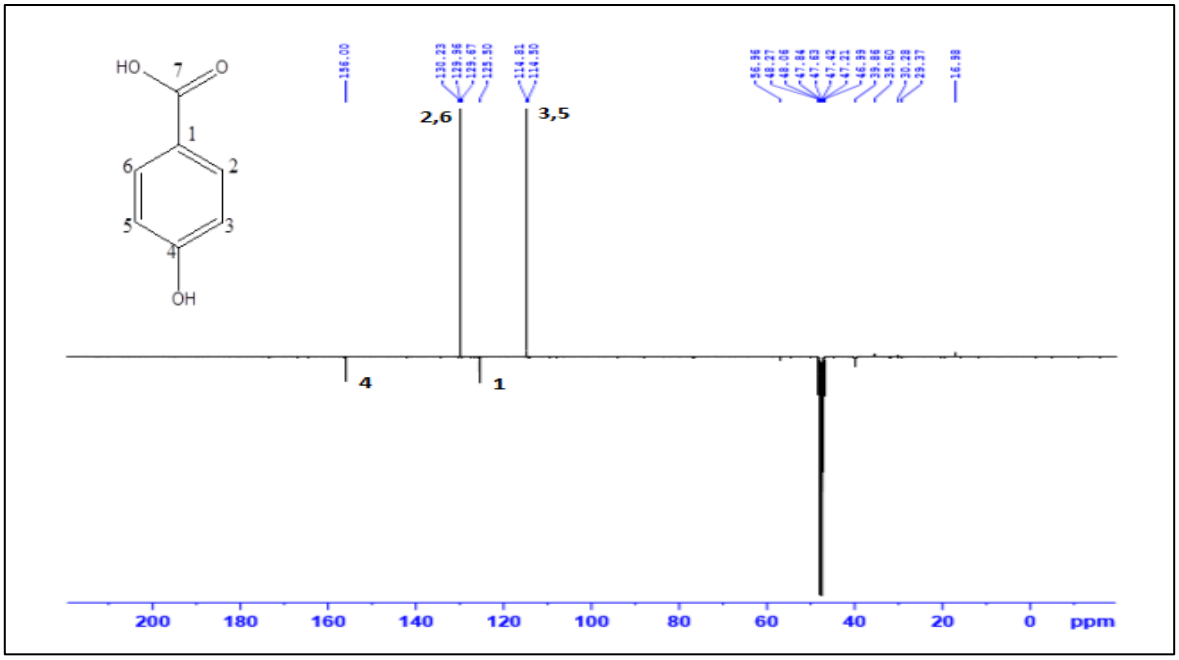

Figure S29: ^{13}C NMR (100MHz) data of compound **10** in CD_3OD

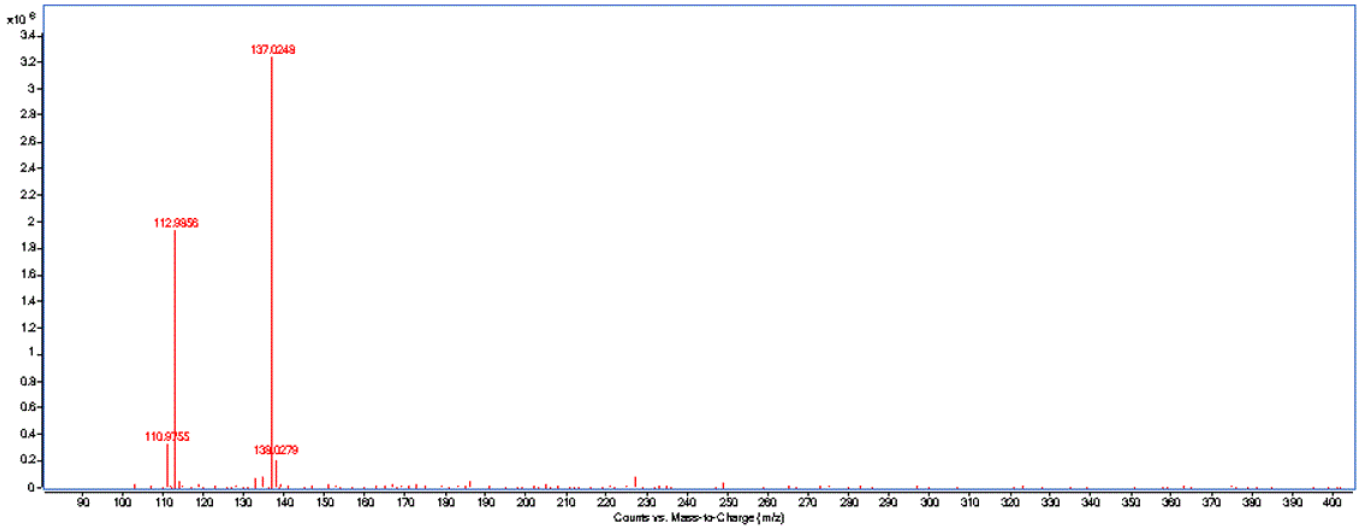

Figure S30: QTOF-HR-ESI-MS analysis (negative mode) of compound **10**

Compound 11:

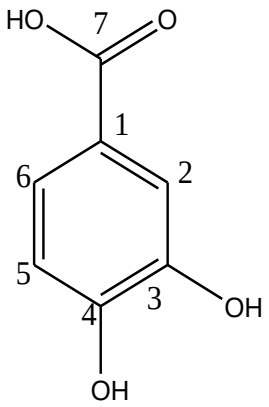

Table S9: ^{1}H (500 MHz) and ^{13}C NMR (125MHz) data of compound **11** in CD_3OD

H/C no.	^{1}H-NMR	^{13}C-NMR	^{13}C-NMR* [12]
1			123.7
2	7.42 (H, *s*)	117.7	117.8
3		146.0	146.0
4		151.4	151.3
5	6.78 (H, *d, J*=8.5*)*	115.7	115.8
6	7.40 (H, bd. *s*)	123.8	123.8
7		ND	170.6

***** ^{1}H and ^{13}C-NMR are measured in CD_3OD at 300 and 75.5 MHz respectively.
ND:Not detected .

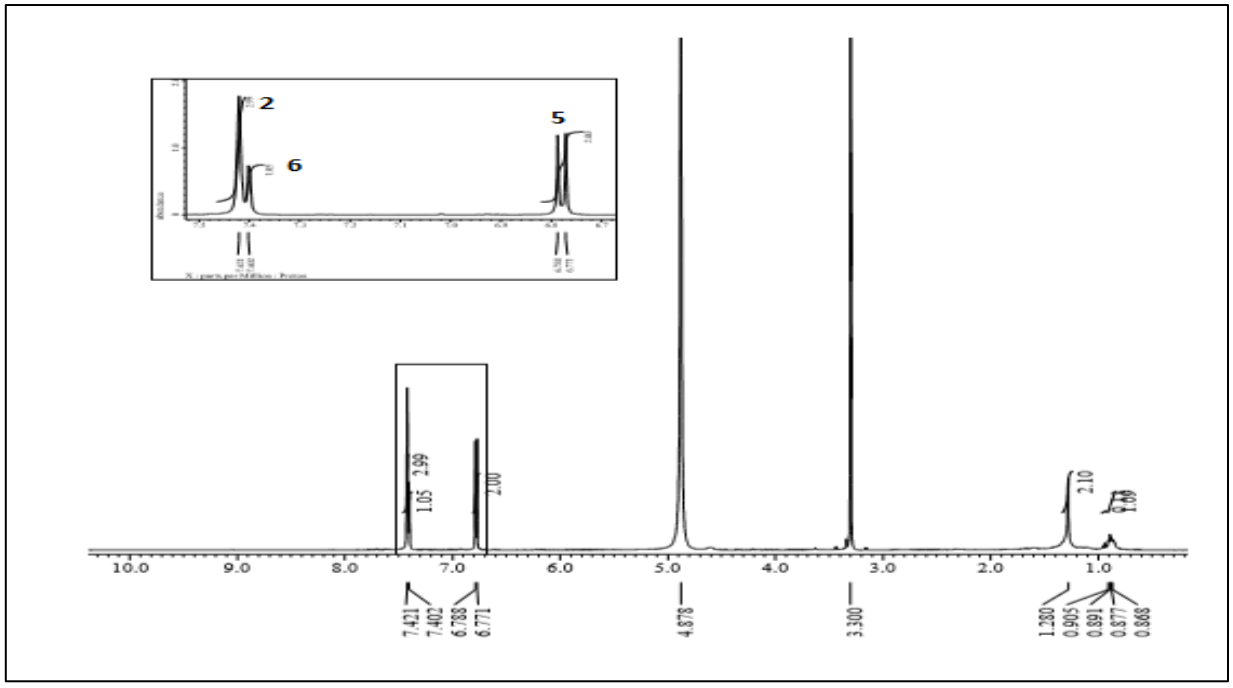

Figure S31: ^{1}H (500 MHz) of compound **11** in CD_3OD

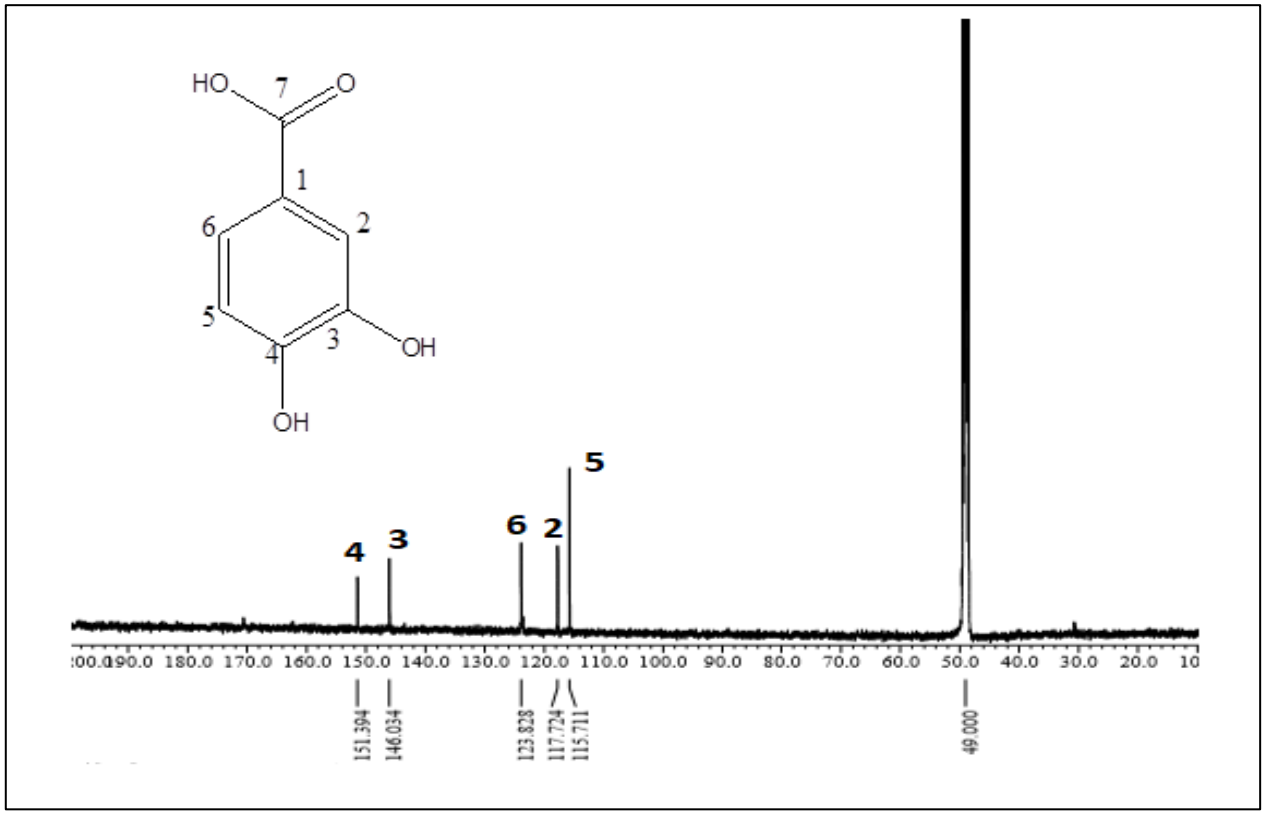

Figure S32: ^{13}C NMR (125MHz) data of compound **11** in CD_3OD

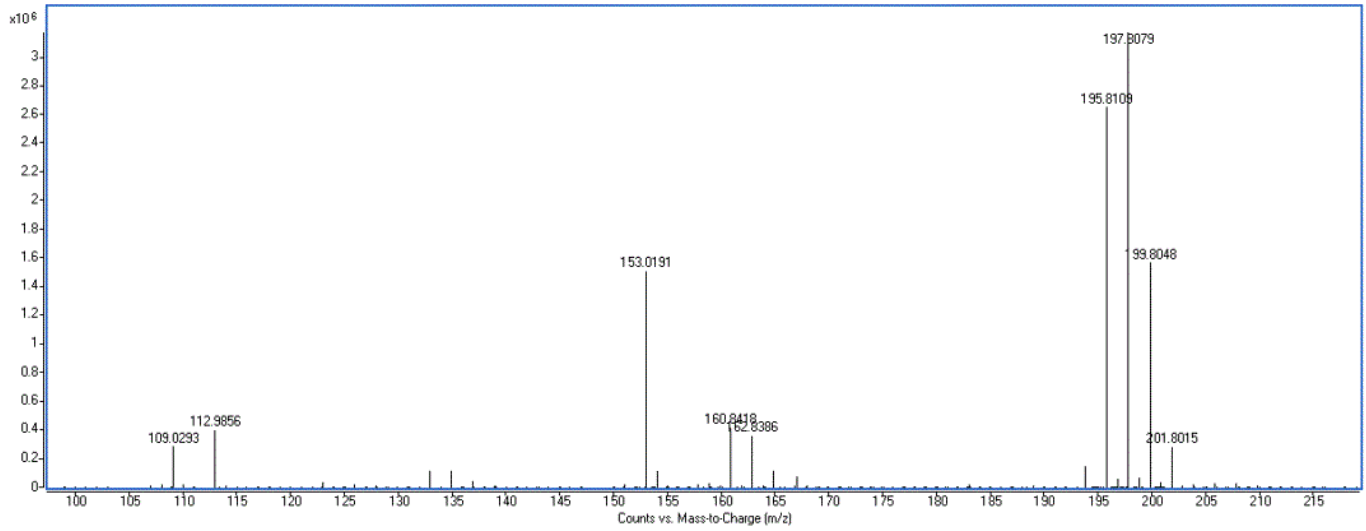

Figure S33: QTOF-HR-ESI-MS analysis (negative mode) of compound **11**

Compound 12:

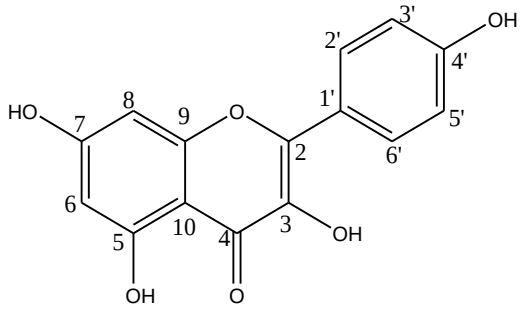

Table S10: ^{1}H (500 MHz) and ^{13}C NMR (125MHz) data of compound **12** in CD_3OD

H/C no.	^{1}H-NMR	^{13}C-NMR	^{1}H-NMR* [13]	^{13}C-NMR** [14]
1				
2		148.9		146.8
3		138.0		136.6
4		178.2		176.6
5		163.3		162.3
6	6.18 (1H, *d*, *J*= 1.5)	100.1	6.15(*s*)	99.2
7		166.4		164.9
8	6.39 (1H, *d*, *J*=1.5)	95.3	6.35 (*s*)	94.4
9		161.4		157.7
10		105.3		104.1
1'		124.5		123.3
2',6'	8.07 (2H, *d*, *J*= 9.0)	131.5	8.05 (2H, *d*, *J*= 8.5)	125.9
3', 5'	6.89 (2H, *d*, *J*= 9.0)	117.1	6.88 (2H, *d*, *J*= 8.5)	116.3
4'		159.1		160.1

*^{1}H-NMR is measured in CD_3OD at 400 MHz.
**^{13}C-NMR is measured in CD_3OD at 125 MHz.

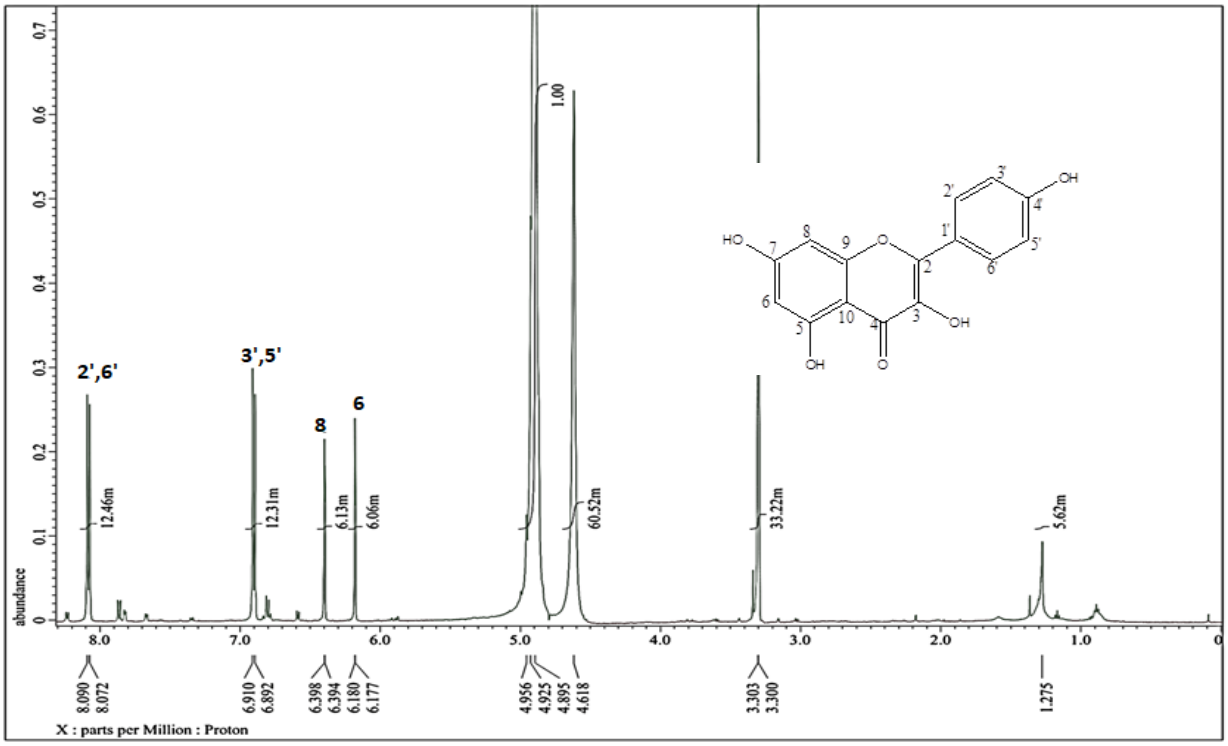

Figure S34: ^{1}H (500 MHz) data of compound **12** in CD_3OD

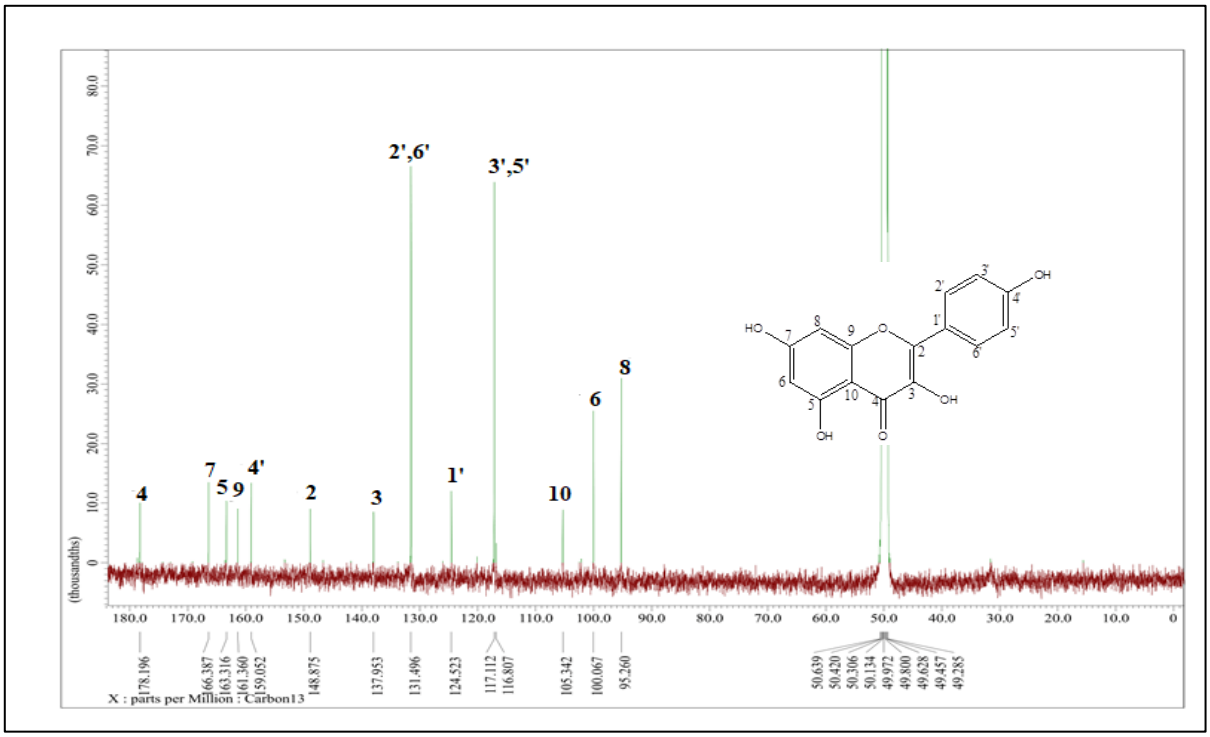

Figure S35: ^{13}C NMR (125MHz) data of compound **12** in CD_3OD

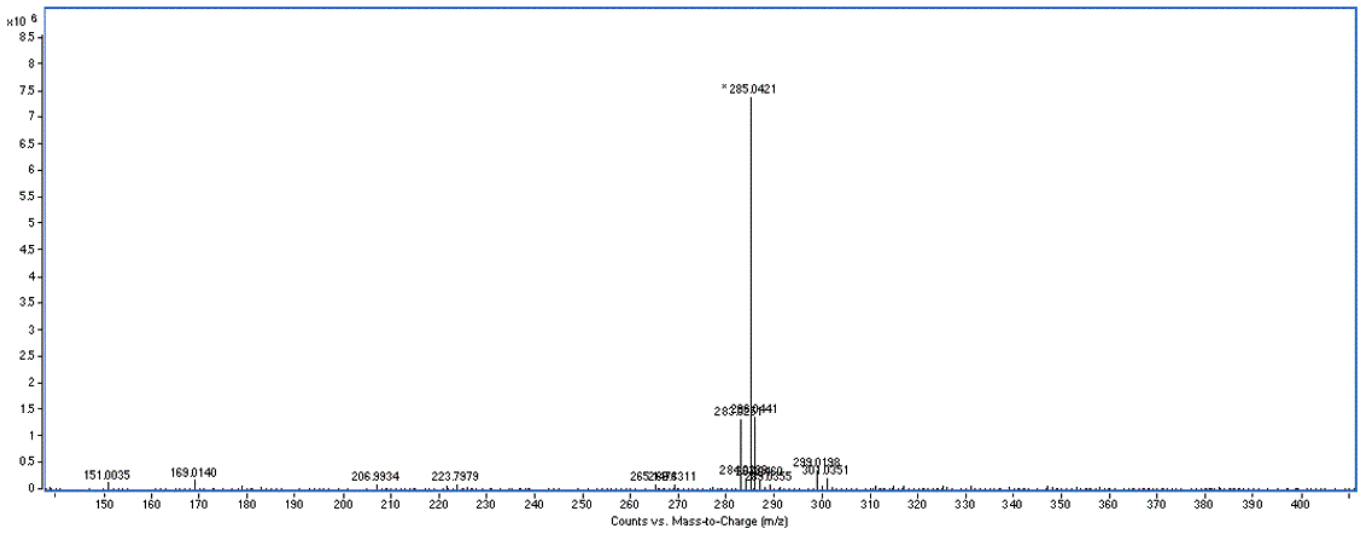

Figure S36: QTOF-HR-ESI-MS analysis (negative mode) of compound **12**

Compound 13:

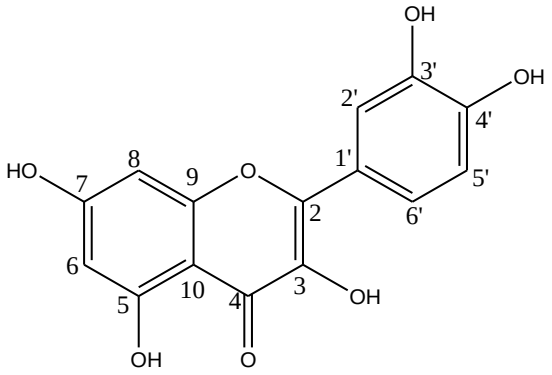

Table S11: ^{1}H (400 MHz) data of compound **13** in CD_3OD

H/C no.	^{1}H-NMR	^{1}H-NMR* [15]
1		
2		
3		
4		
5		
6	6.17 (1H, *d*, *J*=1.5)	6.18 (*d*, *J*=2.03)
7		
8	6.38 (1H, *d*, *J*=2.0)	6.40 (*d*, *J*=2.03)
9		
10		
1'		
2'	7.73 (1H, *d*, *J*=2.0)	7.68 (*d*, *J*= 2.2)
3'		
4'		
5'	6.87 (1H, *d*, *J*=8.5)	6.88 (*d*, *J*= 8.47)
6'	7.62 (1H, *dd*, *J*=9.0, 2.5)	7.54 (*dd*, *J*= 8.5, 2.2)

*^{1}H-NMR is measured in DMSO-*d6* at 60 0MHz

Figure S37: ^{1}H (400 MHz) data of compound **13** in CD_3OD

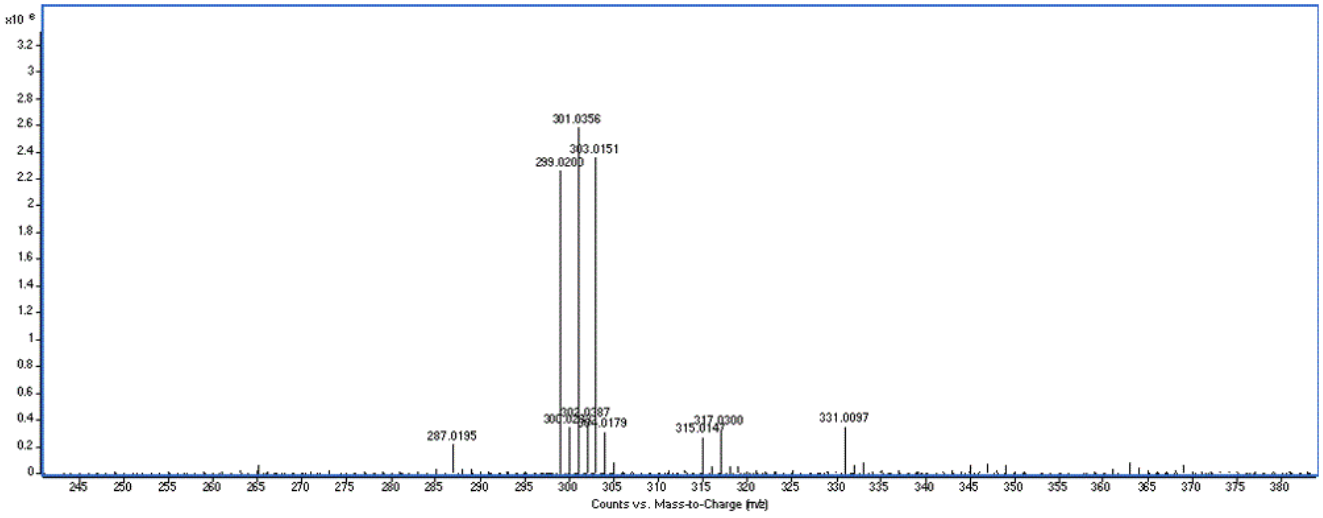

Figure S38: QTOF-HR-ESI-MS analysis (negative mode) of compound **13**

Compound 14

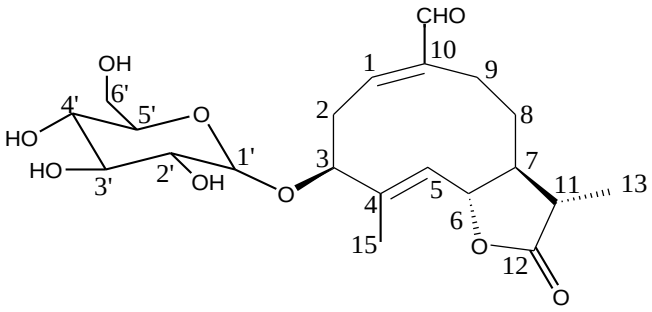

Table S12: ^{1}H (500 MHz) and ^{13}C NMR (125MHz) data of compound **14** in CD_3OD

H/C no.	^{1}H-NMR	^{13}C-NMR	^{1}H-NMR * [16]	^{13}C-NMR*[16]
1	6.56 (1H, *t*, *J*=8.4 HZ)	152.1	6.24 (1H, br. *t*, *J*=8 Hz)	150.1
2	3.54-4.38 (*m*)	33.6	3.90-4.90 (*m*)	32.9
3		80.7		79.8
4		137.7		136.8
5	5.02 (1H, br. *d*, *J*= 10.0 HZ)	128.0	5.04 (1H, br. *d*, *J*=10 Hz)	127.0
6	3.54-4.38 (*m*)	81.9	3.90-4.90 (*m*)	80.2
7		50.5		49.5
8		23.2		22.4
9		26.1		25.5
10		147.0		145.6
11		42.4		41.3
12		181.4		178.5
13	0.97 (3H, *d*, *J*=7.2 HZ)	12.9	1.18 (3H, *d*, *J*=7 Hz)	12.8
14	9.31 (1H, br *s*)	197.8	9.49 (1H, br *s*)	195.6
15	1.86 (3H, br *s*)	11.3	2.14 (3H, br *s*)	11.2
1'	4.12 (1H, *d*, *J*=7.7)	102.0		101.9
2'		75.1		74.9
3'		78.0		78.2
4'		71.8		71.6
5'		78.0		78.2
6'		62.8		62.7

*^{1}H and ^{13}C -NMR are measured in C_5D_5N at 400 and 90 MHz respectively.

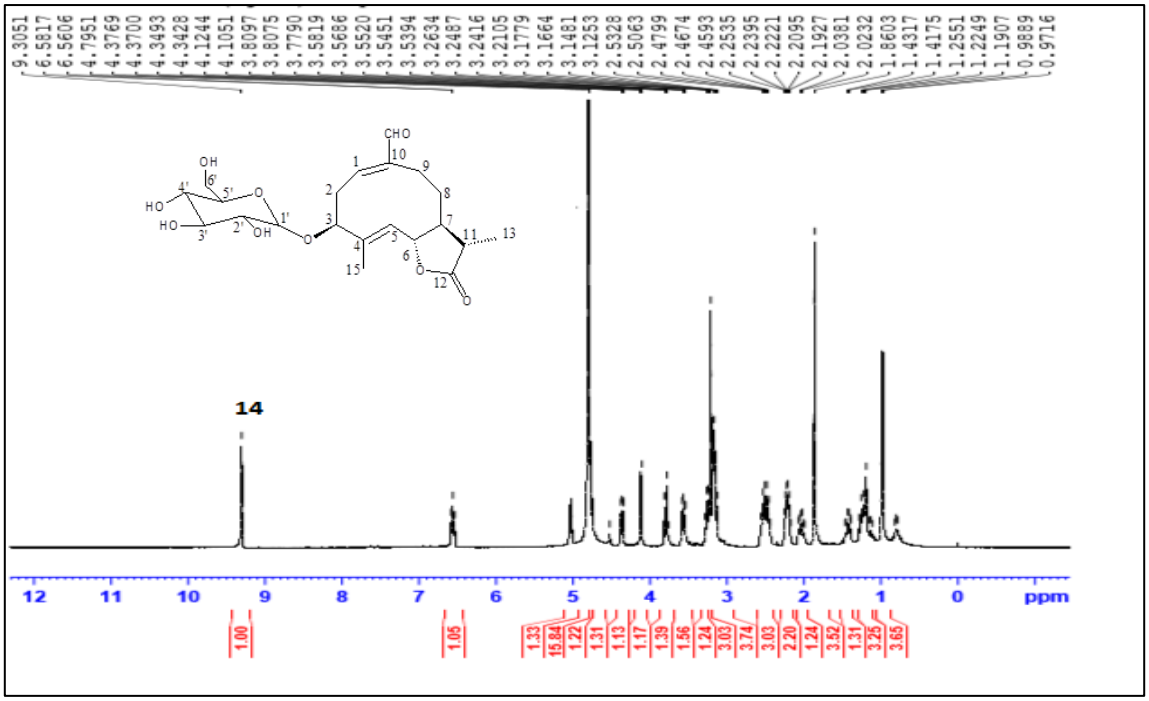

Figure S39: ^{1}H (500 MHz) data of compound **14** in CD_3OD

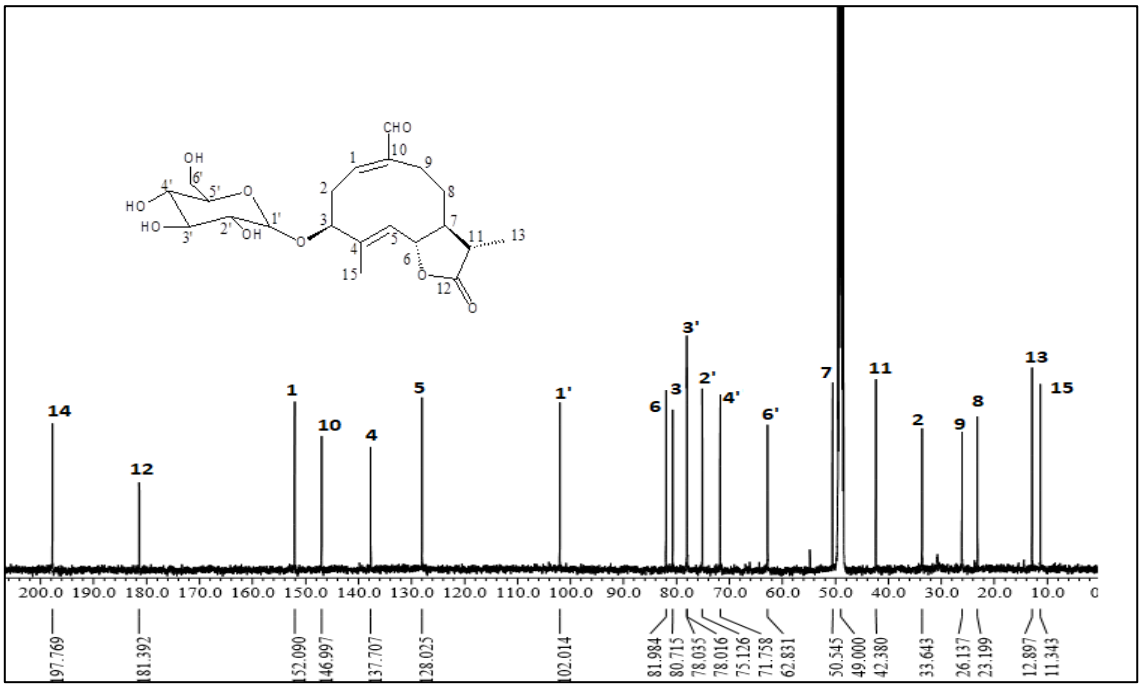

Figure S40: ^{13}C NMR (125MHz) data of compound **14** in CD_3OD

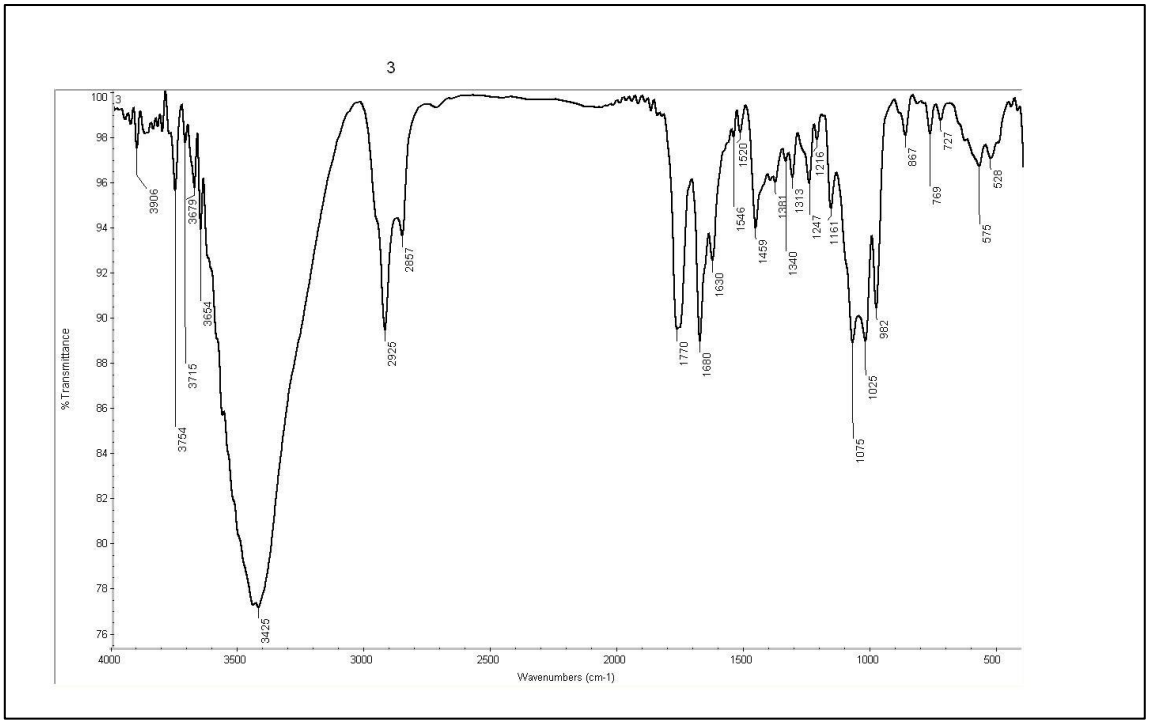

Figure S41: IR spectrum of compound **14** (KBr)

Compound 15

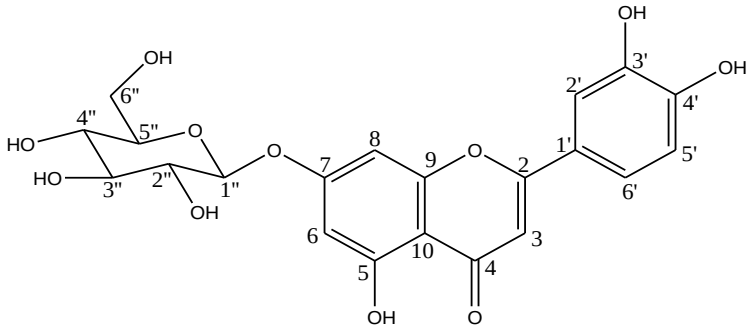

Table 13: ^{1}H (500 MHz) and ^{13}C NMR (125MHz) data of compound **15** in DMSO-d_6

H/C no.	^{1}H-NMR	^{13}C-NMR	^{1}H-NMR * [17]	^{13}C-NMR** [18]
2		164.5		163.6
3	6.75 (1H, *s*)	103.2	6.61 (1H, *s*)	103.7
4		181.9		182.5
5		161.1		161.8
6	6.43 (1H, *d*, *J*= 2.0 Hz)	99.5	6.42 (1H, *d*, *J* = 2.3 Hz)	100.2
7		162.9		165.2
8	6.78 (1H, *d*, *J*= 2.0 Hz)	94.7	6.90 (1H, *d*, *J* = 2.3 Hz)	95.4
9		156.9		157.6
10		105.3		106.0
1'		121.3		121.8
2'	7.41 (1H, *s*)	113.3	7.43 (1H, *d*, *J* = 2.3 Hz)	114.1
3'		145.8		146.6
4'		149.9		151.0
5'	6.90 (1H,*d*, *J*= 8.5 Hz)	116.0	6.92 (1H, *d*, *J* = 8.4 Hz)	116.7
6'	7.43 (1H, *dd*, *J*= 8.0, 2.0 Hz)	119.2	7.40 (1H, *d*, *J* = 2.3, 8.4 Hz)	119.9
1''	5.08 (1H, *d*, *J*= 7.0Hz)	99.8	5.08 (1H, *d*, *J* = 7.65 Hz)	100.6
2''	3.42-3.70	73.1	3.5-4.1	73.8
3''		76.4		77.1
4''		69.5		70.3
5''		77.1		77.8
6''		60.6		61.3

*^{1}H-NMR is measured in DMSO-d_6 at 500 MHz.
**^{13}C-NMR is measured in DMSO-d_6 at 75 MHz.

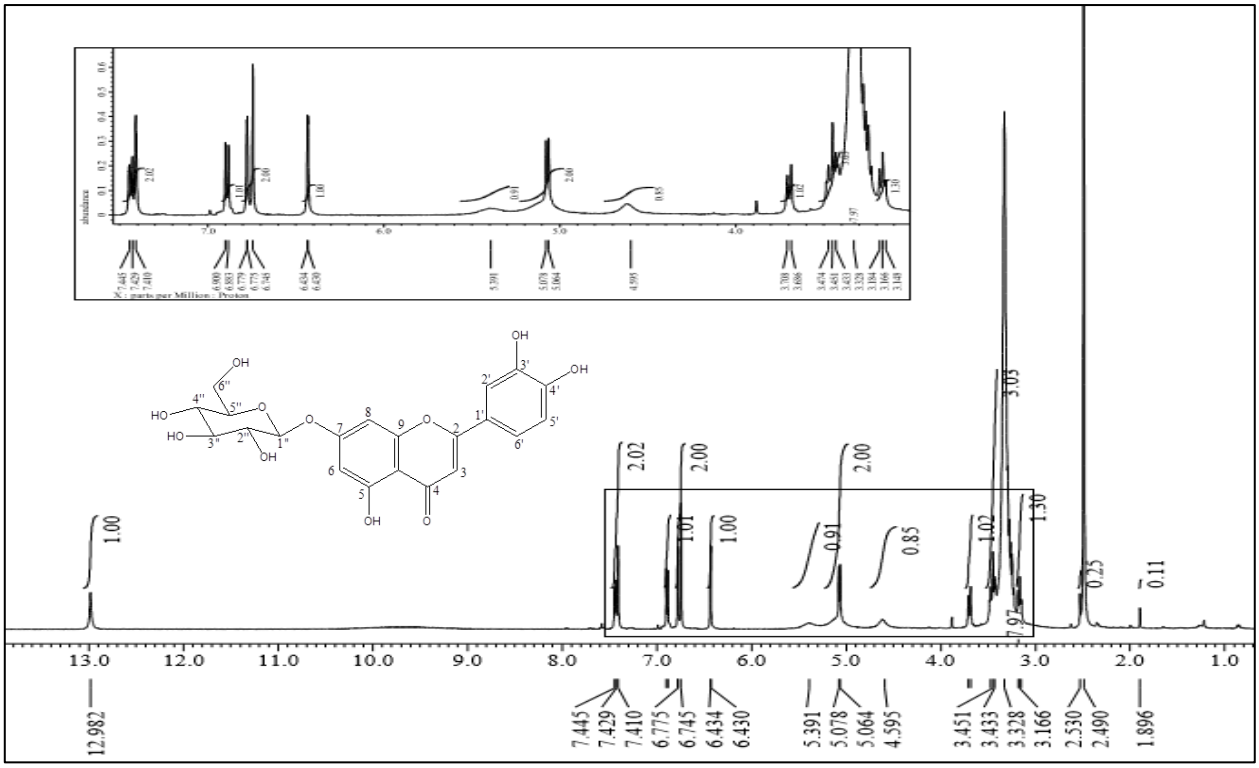

Figure S42: ^{1}H (500 MHz) data of compound **15** in DMSO-d_6

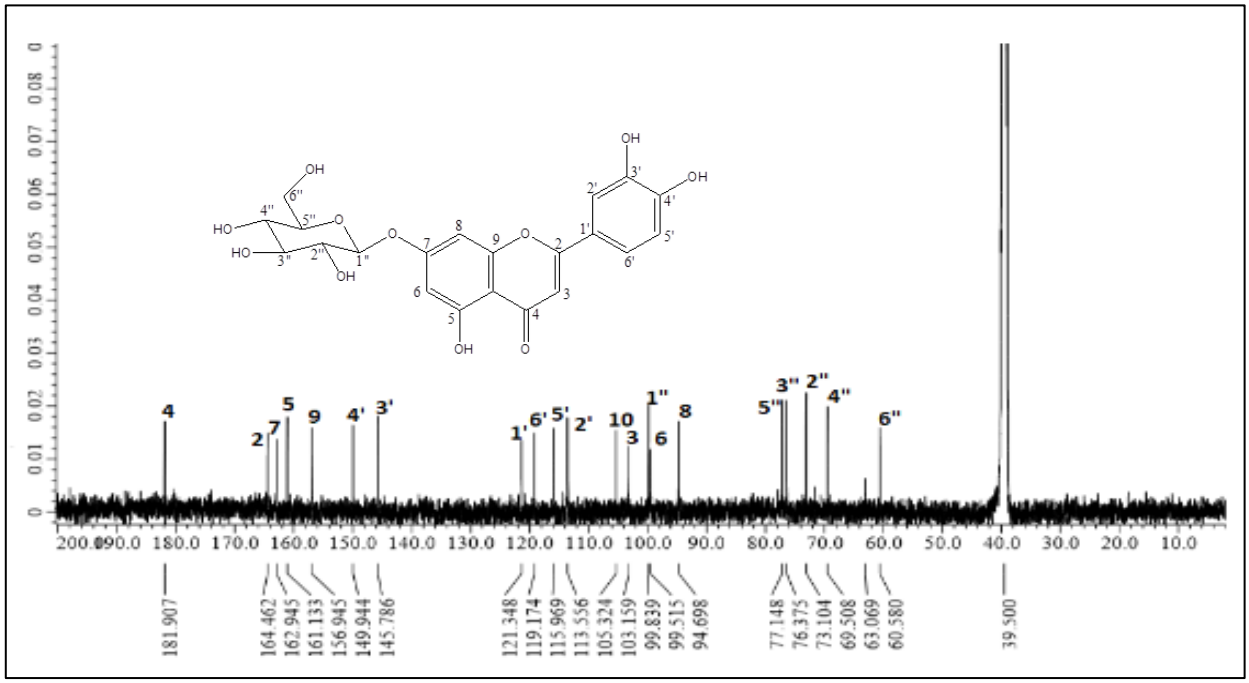

Figure S43: ^{13}C NMR (125MHz) data of compound **15** in DMSO-d_6

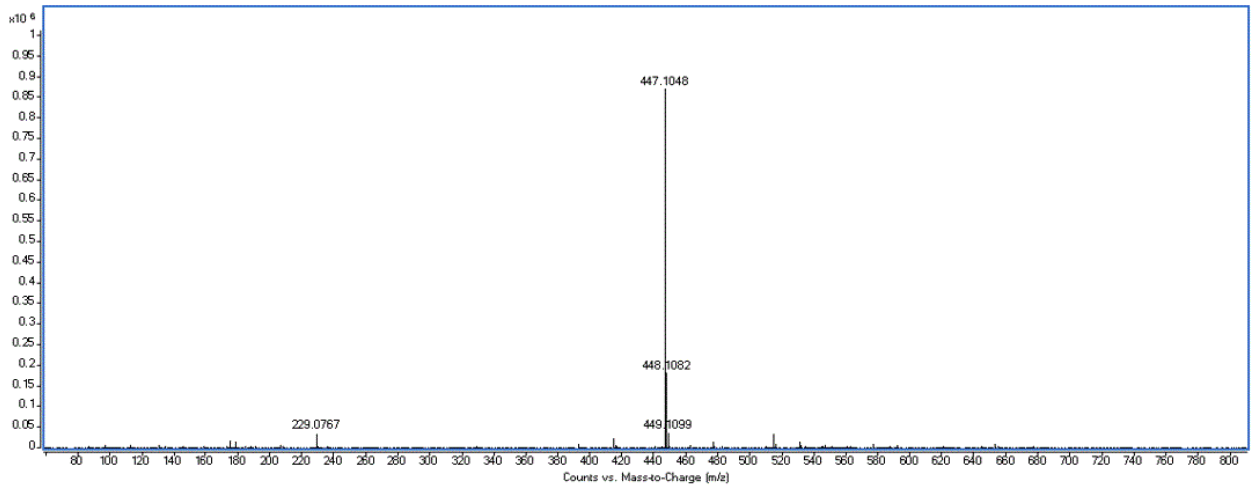

Figure S44: QTOF-HR-ESI-MS analysis (negative mode) of compound **15**

Compound 16

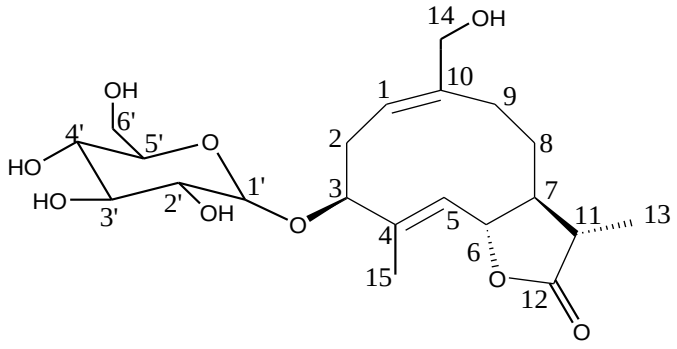

Table S14: ^{1}H (400 MHz) and ^{13}C NMR (100 MHz) data of compound **16** in CD_3OD

H/C no.	^{1}H-NMR	DEPTQ	^{1}H-NMR*[16]	^{13}C-NMR*[16]
1	5.00[a]	127.3	5.10 (1H, *dd*, *J*=13,4 Hz)	127.4
2	2.34[a]	31.9		32.8
3	4.44 (1H, t)[b]	82.6	4.58 (1H, *dd*, *J*= 10, 7 Hz)	83.3
4		140.0		140.6
5	4.95[a]	127.1	4.94 (1H, br. *d*, *J*= 10 Hz)	126.7
6	4.69[a]	81.2	4.86 (1H, t, *J*= 10 Hz)	80.8
7	1.65[a]	54.1		54.5
8	1.63[a] 1.74[a]	27.9		29.0
9	1.77[a] 2.70 (1H, *dd*, *J*=7.5)[b]	35.6		36.8
10		140.6		142.1
11	2.29[a]	41.9		42.3
12		180.0		178.4
13	1.12 (3H, *d*, *J*=6.8 Hz)	12.0	1.26 (3H, *d*, *J*=7 Hz)	13.3
14	3.73[a] 4.13[a]	57.4	4.19 (1H, br. *d*, *J*= 13 Hz) 4.63 (IH, br. *d*, *J*= 13 Hz)	58.6
15	1.57 (3H, br. *s*)	10.3	1.90 (3H, br. *s*)	11.6
1'	4.11 (1H, *d*, *J*= 7.2)	101.1		102.5
2'	3.11-3.79	73.8		75.0
3'		76.6		78.2
4'		70.4		71.7
5'		76.6		78.1
6'		61.4		62.8

[a] Peaks multiplicity is not clear due to overlapping with other peaks.
[b] peaks *J* values cannot be determined due to peaks deformity.
*^{1}H and ^{13}C -NMR are measured in C_5D_5N at 400 and 90 MHz respectively

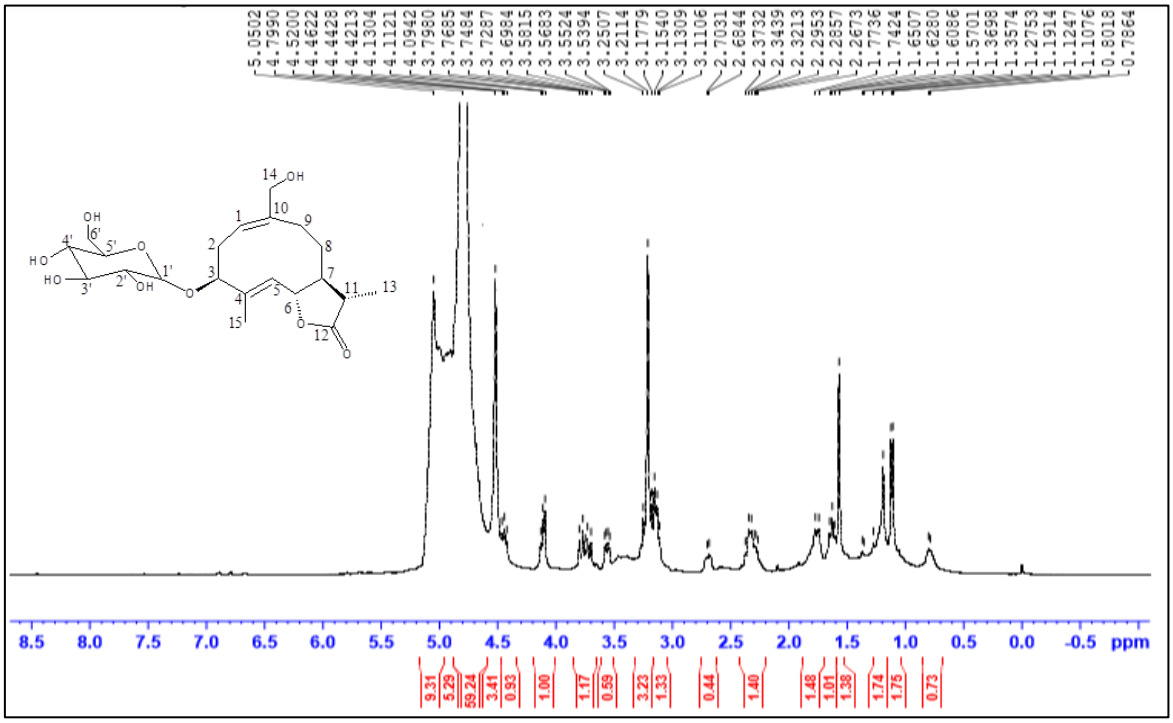

Figure S45: ^{1}H (400 MHz) data of compound **16** in CD_3OD

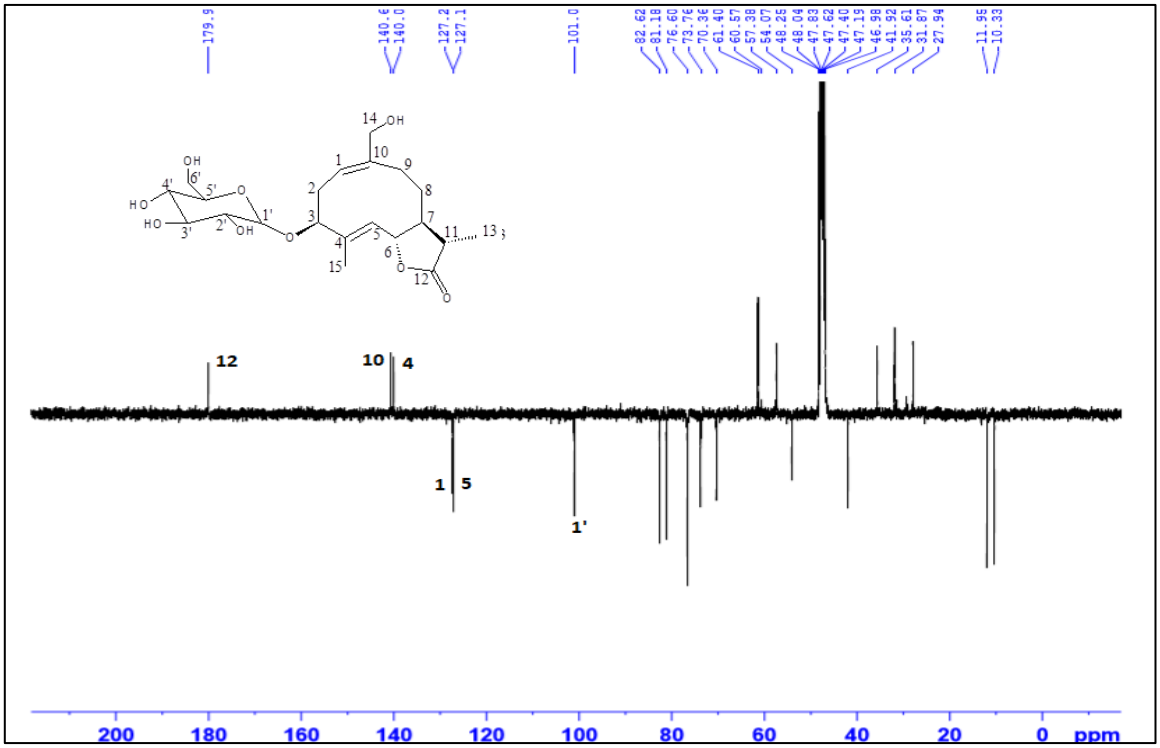

Figure S46: DEPTQ (100 MHz) data of compound **16** in CD_3OD

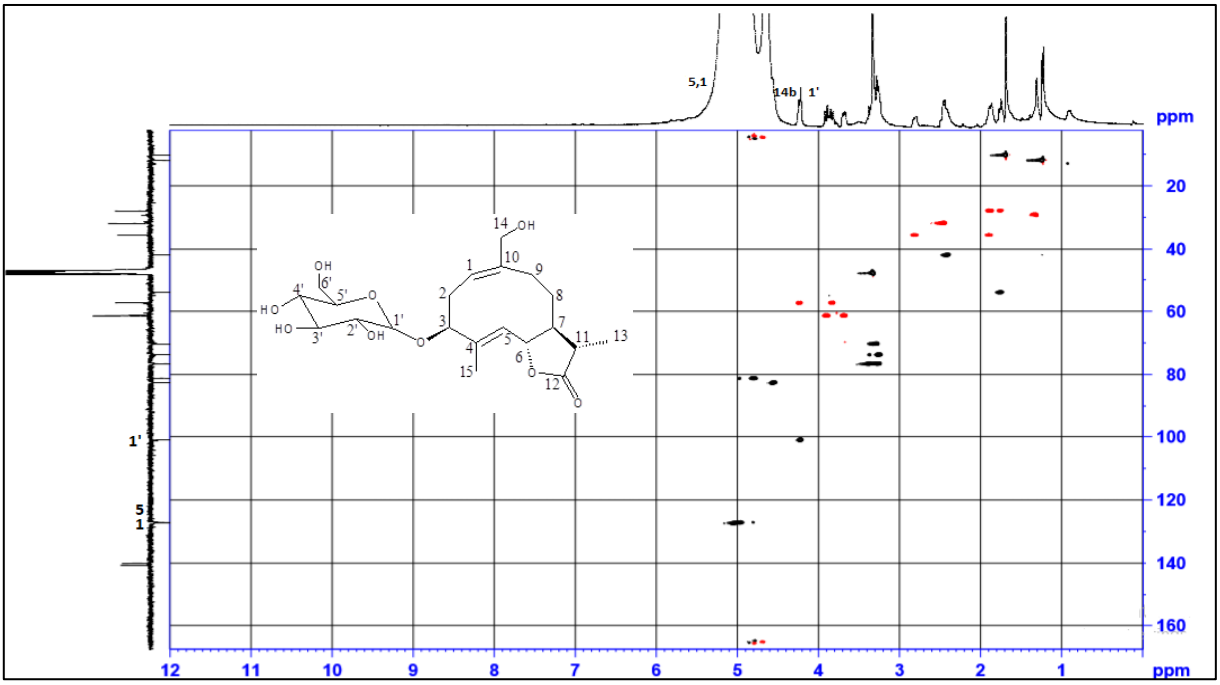

Figure S47: HSQC spectrum of compound **16** in CD_3OD

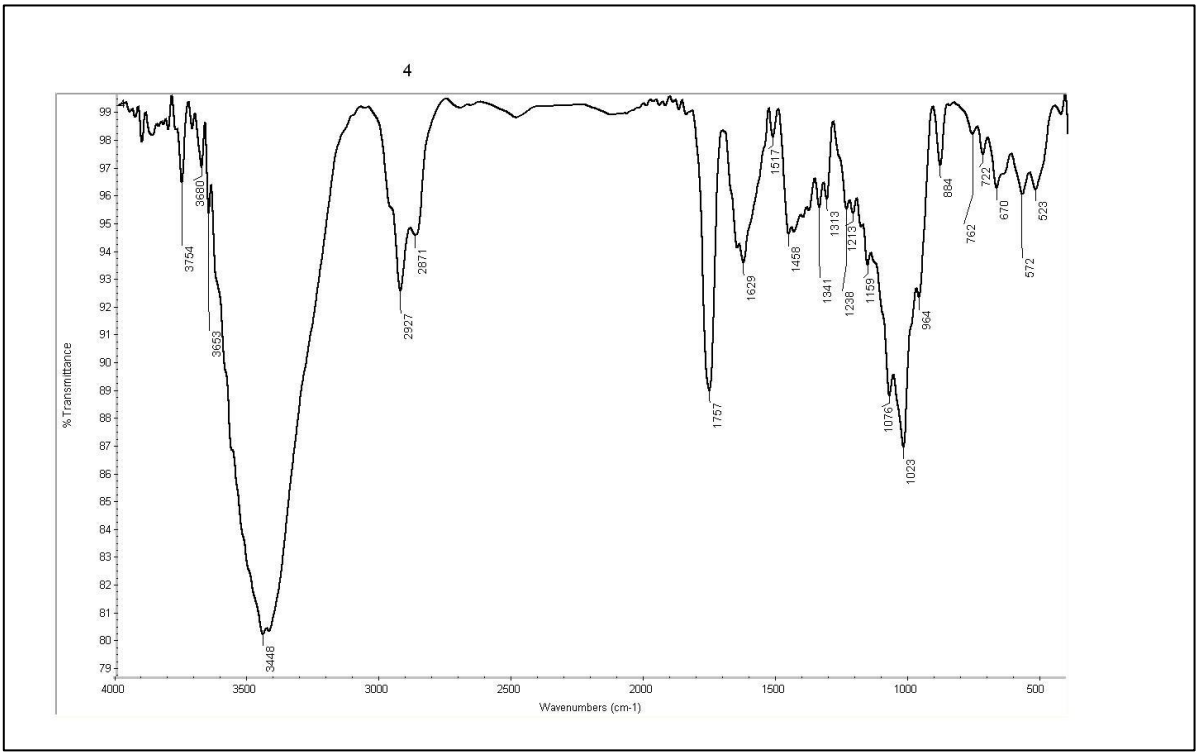

Figure S48: IR spectrum of compound **16** (KBr)

Compound 17

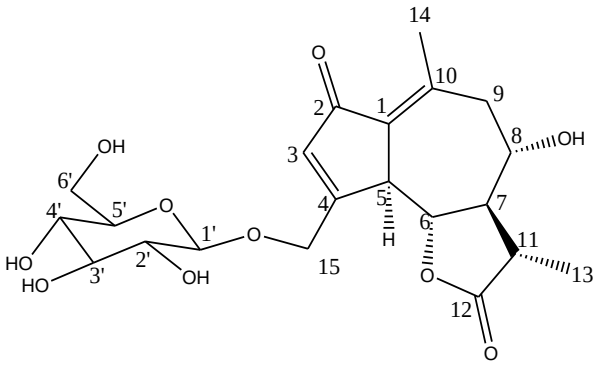

Table S15: ^{1}H (400 MHz) and DEPTQ (100 MHz) data of compound **17** in CD_3OD

H/C no.	^{1}H-NMR	DEPTQ	Type	^{1}H-NMR* [11]	^{13}C-NMR* [11]
1		132.1	Q		132.1
2		196.1	Q		196.1
3	6.56 (1H, br. *s*)	133.3	CH	6.57 (1H, br. *s*)	134.4
4		170.5	Q		169.4
5	3.74[b]	48.6	CH	3.61 (*d*, *J*=10)	49.3
6	3.76[b]	81.2	CH	3.65 (*dd*, *J*=10, 10)	81.4
7	2.18 (1H, *dd*, *J*=10.0)[a]	60.8	CH	2.15 (*ddd*, *J*=12,10, 9.6)	61.3
8	3.67 (1H, *m*)	68.6	CH	3.81 (*m*)	69.0
9	2.39 (1H, *dd*, *J*= 11.2,1.6) 2.81(1H, *dd*, *J*=10.8)[a]	48.3	CH_2	2.42 (*dd*, *J*=13.6,2.0) 2.78 (*dd*, *J*= 13.6, 10.8)	49.4
10		148.7	Q		149.3
11	2.65 (*dd*, *J*= 5.6)[a]	41.1	CH	2.59 (*dq*, *J*= 12, 7.2)	41.8
12		178.7	Q		178.9
13	1.40 (1H, *d*, *J*=6.8)	14.4	CH_3	1.43 (*d*, *J*=7.2)	15.3
14	2.44 (1H, *s*)	20.4	CH_3	2.44 (br. *s*)	21.9
15	4.76 [b] 4.81[b]	68.2	CH_2	4.76 (*d*, *J*=17.2), 4.85 (*d*, *J*= 17.2)	68.7
1'	4.40 (*d*, *J*=7.6)	102.7	CH	4.40 (*d*, 8.0)	102.8
2'	3.26 (1H, *m*)	73.7	CH	3.32 *m*	73.8
3'	3.38(1H, *m*)	76.6	CH	3.45 *m*	76.4
4'	3.32(1H, *m*)	70.2	CH	3.36 *m*	70.3
5'	3.38(1H, *m*)	76.6	CH	3.44 *m*	76.7
6'	3.70[b] 3.91 (1H, *J*=11.6)	61.3	CH_2	3.76 (*dd*, 12.0, 4.8), 3.89 (*dd*, 12.0, 2.0)	61.8

[b] Peaks multiplicity is not clear due to overlapping with other peaks.

[a] peaks *J* values cannot be determined due to peaks deformity.

*^{1}H and ^{13}C -NMR are measured in CD_3OD at 400 and 100 MHz respectively.

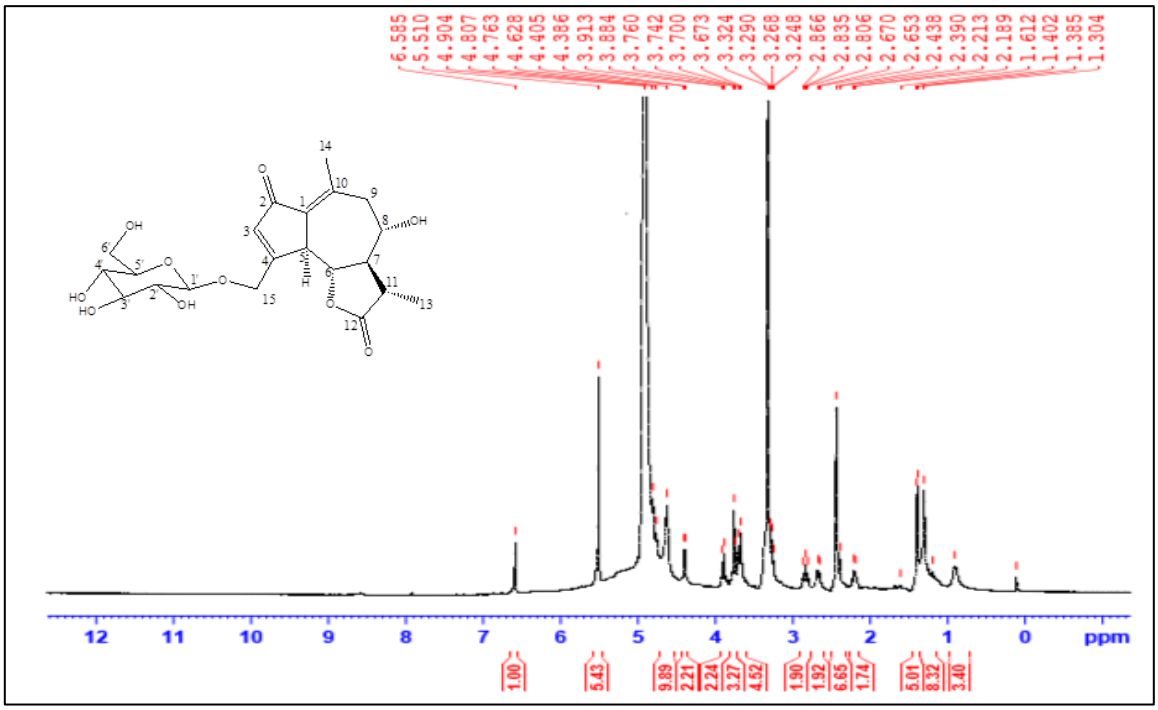

Figure S49: ^{1}H (400 MHz) data of compound **17** in CD_3OD

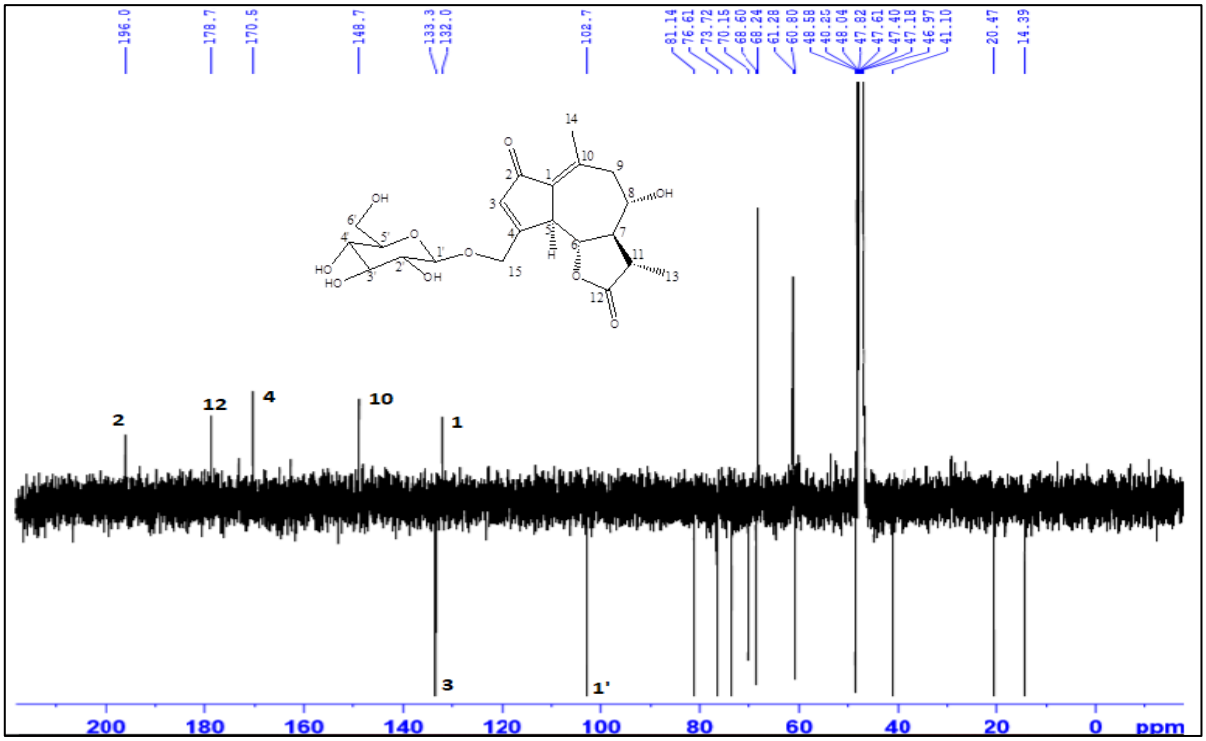

Figure S50: DEPTQ (100 MHz) data of compound **17** in CD_3OD

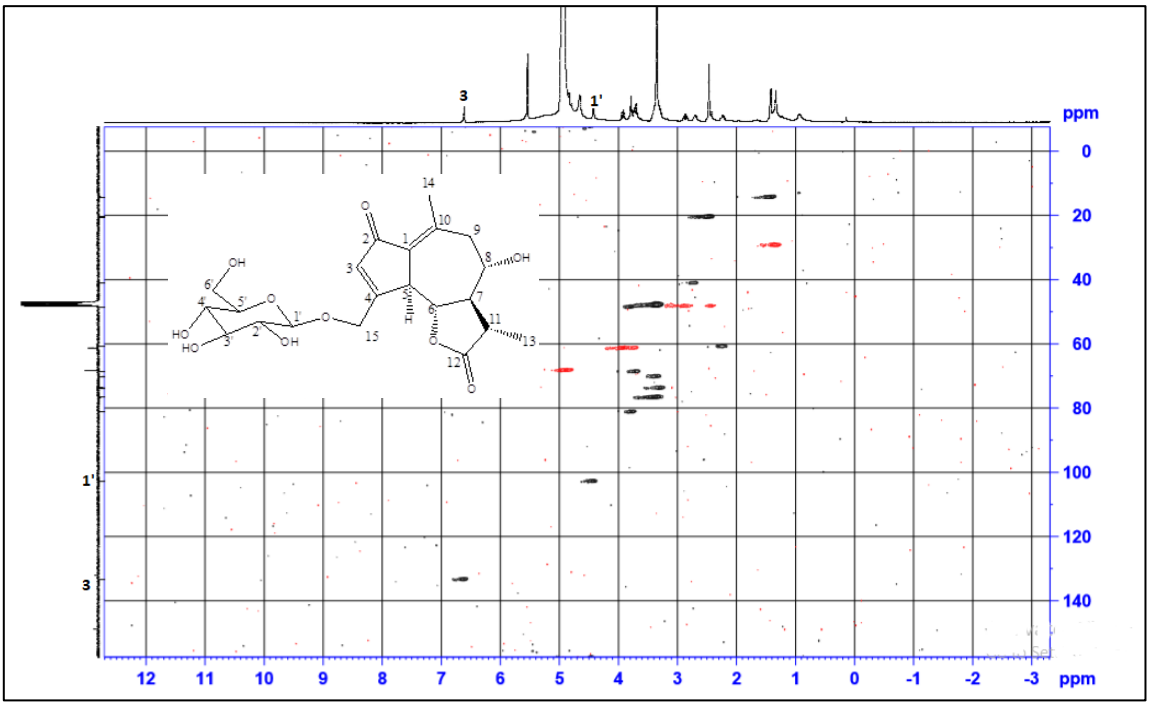

Figure S51: HSQC spectrum of compound **17** in CD_3OD

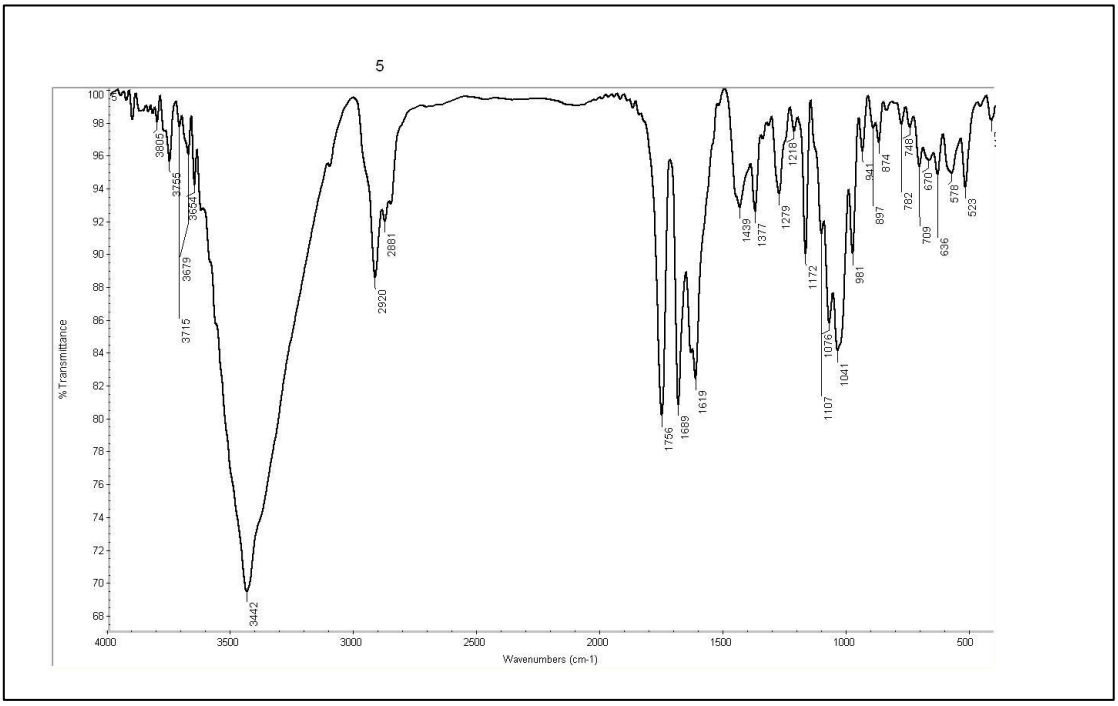

Figure S52: IR spectrum of compound **17** (KBr)

References

[1] L. Shai, S. Magano, S. Lebelo and A. Mogale (2011). Inhibitory effects of five medicinal plants on rat alpha-glucosidase: Comparison with their effects on yeast alpha-glucosidase, *J. Med. Plants Res*. **5**, 2863-2867.

[2] R. Re, N. Pellegrini, A. Proteggente, A. Pannala, M. Yang and C. Rice-Evans (1999). Antioxidant activity applying an improved ABTS radical cation decolorization assay, *Free Radic. Biol. Med*. **26**, 1231-1237.

[3] R. Boly, T. Lamkami, M. Lompo, J. Dubois and I. Guissou (2016). DPPH free radical scavenging activity of two extracts from *Agelanthus dodoneifolius* (Loranthaceae) leaves, *Int. J. Toxicol. Pharmacol. Res*. **8**, 29-34.

[4] I. F. Benzie and J. J. Strain (1996). The ferric reducing ability of plasma (FRAP) as a measure of "antioxidant power": the FRAP assay, *Anal. Biochem*. **239**, 70-76.

[5] A. T. M. Silva, C. G. Magalhães, L. P. Duarte, W. D. N. Mussel, A. L. T. G. Ruiz, L. Shiozawa, J. E. D. Carvalho, I. C. Trindade and S. A. Vieira Filho (2018). Lupeol and its esters: NMR, powder XRD data and *in vitro* evaluation of cancer cell growth, *Braz. J. Pharm. Sci.* **53.**

[6] J. Dai, C. Zhao, Q. Zhang, Z.-L. Liu, R. Zheng and L. Yang (2001). Taraxastane-type triterpenoids from *Saussurea petrovii*, *Phytochemistry*. **58**, 1107-1111.

[7] C.-C. Yu, Y.-S. Lee, B.-S. Cheon and S.-H. Lee (2003). Synthesis of glycerol monostearate with high purity, *B. Korean Chem. Soc*. **24**, 1229-1231.

[8] M. H. Oueslati, Z. Mighri, H. B. Jannet and P. M. Abreu (2005). New ceramides from *Rantherium suaveolens*, *Lipids*. **40**, 1075-1079.

[9] Y. Ren, Y. Zhou, X. Chen and Y. Ye (2005). Discovery, structural determination and anticancer activities of lactucinlike guaianolides, *Lett. Drug Des. Discov*. **2**, 444-450.

[10] T. Rho and K. D. Yoon (2017). Chemical constituents of *Nelumbo nucifera* seeds, *Nat. Prod. Sci*. **23**, 253-257.

[11] Y.-F. Han, G.-X. Cao, X.-J. Gao and M. Xia (2010). Isolation and characterisation of the sesquiterpene lactones from *Lactuca sativa* L. *var*. *anagustata*, *Food Chem*. **120**, 1083-1088.

[12] D. Gutzeit, V. Wray, P. Winterhalter and G. Jerz (2007). Preparative isolation and purification of flavonoids and protocatechuic acid from sea buckthorn juice concentrate (*Hippophaë rhamnoides* L. ssp. *rhamnoides*) by high-speed counter-current chromatography, *Chromatographia* **65**, 1-7.

[13] G. Ren, J. Hou, Q. Fang, H. Sun, X. Liu, L. Zhang and P. G. Wang (2012). Synthesis of flavonol 3-*O*-glycoside by UGT78D1, *Glycoconj. J*. **29**, 425-432.

[14] L. S. Aisyah, Y. F. Yun, T. Herlina, E. Julaeha, A. Zainuddin, I. Nurfarida, A. T. Hidayat, U. Supratman and Y. Shiono (2017). Flavonoid compounds from the leaves of *Kalanchoe prolifera* and their cytotoxic activity against P-388 murine leukimia cells, *Nat. Prod. Sci*. **23**, 139-145.

[15] J. G. Napolitano, D. C. Lankin, S. N. Chen and G. F. Pauli (2012). Complete ^{1}H NMR spectral analysis of ten chemical markers of *Ginkgo biloba*, *Magn. Reson. Chem*. **50**, 569-575.

[16] K. Nishimura, T. Miyase, A. Ueno, T. Noro, M. Kuroyanagi and S. Fukushima (1986). Sesquiterpene lactones from *Lactuca laciniata*, *Phytochemistry* **25**, 2375-2379.

[17] R. Mohammed, A. A. Zeid, S. El Hawary, A. Sleem and W. Ashour (2014). Flavonoid constituents, cytotoxic and antioxidant activities of *Gleditsia triacanthos* L. leaves, *Saudi J. Biol. Sci*. **21**, 547-553.

[18] M. M. Salama, S. M. Ezzat and A. A. Sleem (2011). A new hepatoprotective flavone glycoside from the flowers of *Onopordum alexandrinum* growing in Egypt, *Z. Naturforsch.C*. **66**, 251-259.